Electronic Supplementary Material (ESI) for ChemComm.

Long-lived Photoluminescence from an Eight-Coordinate Zirconium(IV) Complex with Four 2-(2'-Pyridyl)pyrrolide Ligands

*Dylan C. Leary, Novruz G. Akhmedov, Jordan C. Martinez, Jeffrey L. Petersen, Carsten Milsmann**

C. Eugene Bennett Department of Chemistry, West Virginia University, Morgantown, WV, USA.

camilsmann@mail.wvu.edu

Supporting Information

Contents

1. Materials

All air- and moisture-sensitive manipulations were carried out using standard Schlenk line and cannula techniques or in an MBraun inert atmosphere drybox containing an atmosphere of purified nitrogen. Solvents for air- and moisture-sensitive manipulations were dried and deoxygenated using a Glass Contour Solvent Purification System and stored over 4 Å molecular sieves. All synthesized solids were dried under high vacuum, all liquids were deoxygenated prior to bringing them into the glovebox. Deuterated benzene (C_6D_6) and toluene (C_7D_8) for NMR spectroscopy were distilled from sodium metal while deuterated chloroform was dried over calcium hydride. Tetrabenzyl zirconium[1] and 2-(2'-pyrrolyl)pyridine[2] (H^HPMP^H) were synthesized according to literature procedures. All other chemicals were purchased from commercial sources and used as received.

2. General Considerations for Physical Characterization

Electronic absorption spectra were recorded using a Shimadzu UV-1800 spectrophotometer in gastight quartz cuvettes with a 1 cm path length fitted with J-Young valves. Room-temperature steady-state emission spectra were obtained in 1 cm path length gastight quartz cuvettes with J-Young valves using a

Shimadzu RF-5301 PC spectrofluorophotometer. Frozen solution emission spectra were recorded in quartz EPR tubes fitted with J-Young valves using an Ocean Optics Flame Miniature Spectrometer and a fluorescent light bulb (λ_{max} = 370 nm) as the light source. Time-resolved emission data were collected using a Horiba Jobin Yvon Fluorolog-3 Spectrofluorometer equipped with a single photon counting module in multi-channel scaler mode and either a 456 nm SpectraLED or 454 nm NanoLED pulsed excitation light source. Emission lifetimes were determined by manually fitting the decay traces using the Origin software package. ^{1}H and ^{13}C {^{1}H} NMR spectra were recorded on a Varian INOVA 600 MHz spectrometer. All chemical shifts are reported relative to $SiMe_4$ using ^{1}H (residual) chemical shifts of the solvent as a secondary standard. Elemental analyses were performed at Robertson Microlit Laboratories, Inc., in Ledgewood, NJ.

3. Synthetic Protocols

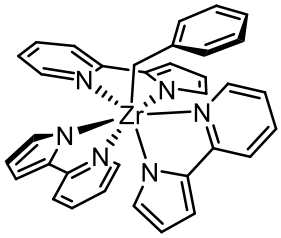

Tetrabenzyl zirconium (100 mg, 1 equiv) and $H^{H}PMP^{H}$ (104 mg, 3.3 equiv) were loaded into an oven-dried 50 mL thick-walled glass vessel in the glovebox. Approximately 5 mL of benzene and a stir bar were added. The thick-walled vessel was sealed with a PTFE screw cap and the yellow-orange solution heated to 90 °C for 16 hours while protected from light. After cooling to room temperature, the reaction vessel was brought back into the glovebox and the solvent removed *in vacuo*. The resulting solid was triturated three times with diethyl ether, dissolved in a minimum amount of THF and filtered through a Celite cake on a medium porosity frit. The filtrate was dried *in vacuo* to provide a yellow-orange powder which was recrystallized from THF/pentane at -35 °C. The final product was isolated on a medium porosity frit as a yellow-orange microcrystalline solid (120 mg, 90%). Single crystals suitable for X-ray diffraction were obtained by slow diffusion of hexanes into a concentrated THF solution at -35 °C. ^{1}H NMR (600 MHz, C_7D_8, 60 °C) δ 7.31 (br s, 3H), 6.93 (d, 3H, ^{3}J = 8.4 Hz), 6.86 (br s, 3H), 6.79 (t, 2H, ^{3}J = 7.8 Hz), 6.74 (t, 3H, ^{3}J = 7.2 Hz), 6.62 (t, 1H, ^{3}J = 7.8 Hz), 6.48 (d, 2H, ^{3}J = 7.2 Hz), 6.26 (br s, 3H), 6.00 (t, 3H, ^{3}J = 6.6 Hz) ppm. ^{13}C{^{1}H} NMR (151 MHz, C_7D_8, 25 °C) δ 155.2, 150.3, 149.1, 140.0, 138.6, 134.5, 128.1, 127.0, 121.3, 118.3, 116.9,

112.3, 110.9, 79.1 ppm. Repeated attempts to obtain satisfactory elemental analysis were unsuccessful. We attribute this to the compound's high sensitivity to air, moisture, and especially light.

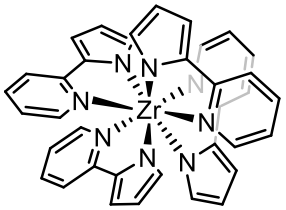

Tetrakis(dimethylamido)zirconium (50 mg, 1 equiv) and $H^{H}PMP^{H}$ (110 mg, 4.1 equiv) were loaded into an oven-dried 50 mL thick-walled glass vessel in the glovebox. Approximately 5 mL of toluene was added EXCLUDING a stir bar. The thick-walled vessel was sealed with a PTFE screw cap and the yellow-orange solution heated to 120 °C for 16 hours. During the reaction, the product formed as single crystals suitable for X-ray diffraction. After cooling to room temperature, the reaction vessel was brought back into the glovebox and the crystalline material was isolated on a medium porosity frit and washed with three 5 mL portions of THF. The product was obtained as yellow-orange crystals (118 mg, 88%). ^{1}H NMR (600 MHz, $CDCl_3$, 25 °C): δ 7.38 (ddd, 1H, ^{3}J = 8.1 Hz, ^{3}J = 7.3 Hz, ^{4}J = 1.6 Hz, pyridine-*H*), 7.32 (ddd, 1H, ^{3}J = 8.1 Hz, ^{4}J = 1.3 Hz, ^{5}J = 0.8 Hz, pyridine-*H*), 6.63 (dd, 1H, ^{3}J = 3.3 Hz, ^{4}J = 1.2 Hz, pyrrole-*H*), 6.50 (ddd, 1H, ^{3}J = 7.3 Hz, ^{3}J = 5.9 Hz, ^{4}J = 1.3 Hz, pyridine-*H*), 6.26 (ddd, 1H, ^{3}J = 5.9 Hz, ^{4}J = 1.6 Hz, ^{5}J = 0.8 Hz, pyridine-*H*), 6.11 (dd, 1H, ^{3}J = 2.2 Hz, ^{4}J = 1.2 Hz, pyrrole-*H*), 6.01 (dd, 1H, ^{3}J = 3.3 Hz, ^{3}J = 2.2 Hz, pyrrole-*H*) ppm. $^{13}C\{^{1}H\}$ NMR (151 MHz, $CDCl_3$, 25 °C, ppm): δ 154.5, 149.0, 140.3, 137.9, 133.2, 119.0, 116.9, 111.2, 109.8 ppm. Anal. Calcd for $C_{36}H_{28}N_8Zr$: C, 65.13; H, 4.25; N, 16.88. Found: C, 64.96; H, 3.65; N, 16.79.

4. X-Ray Crystallography

Single crystals suitable for X-ray diffraction were coated with polyisobutylene oil (Sigma-Aldrich) in a drybox, mounted on a nylon loop, and then quickly transferred to the goniometer head of a Bruker AXS D8 Venture fixed-chi X-ray diffractometer equipped with a Triumph monochromator, a Mo Kα radiation source (λ = 0.71073 Å), and a PHOTON 100 CMOS detector. The samples were cooled to 100 K with an Oxford Cryostream 700 system and optically aligned. The APEX3 software program (version 2016.9-0) was used for diffractometer control, preliminary frame scans, indexing, orientation matrix calculations, least-squares refinement of cell parameters, and the data collection. Three sets of 12 frames each were collected using the omega scan method with a 10 s exposure time. Integration of these frames followed by reflection indexing and least-squares refinement produced a crystal orientation matrix for the crystal lattice that was used for the structural analysis. The data collection strategy was optimized for completeness and redundancy using the Bruker COSMO software suite. The space group was identified, and the data were processed using the Bruker SAINT+ program and corrected for absorption using SADABS. The structures were solved using direct methods (SHELXS) completed by subsequent Fourier synthesis and refined by full-matrix least-squares procedures using the programs provided by SHELXL-2014.

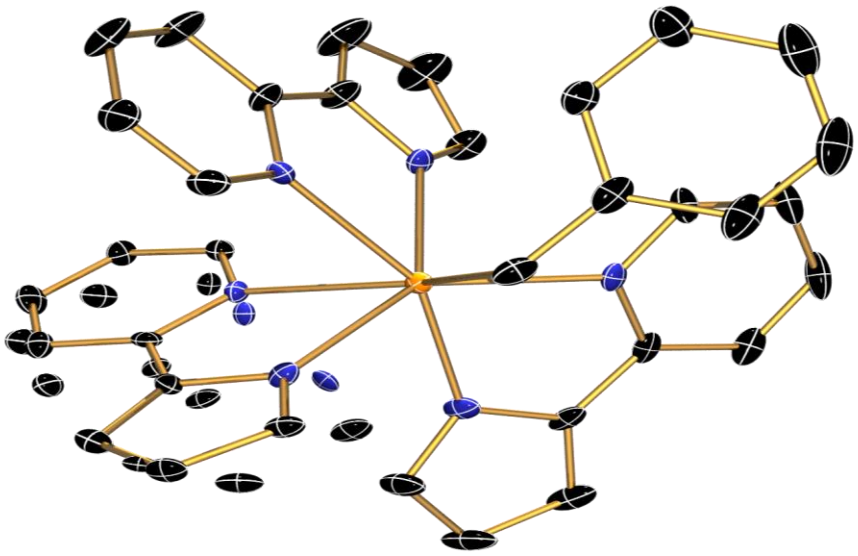

Figure S1. Structure of $Zr(^{H}PMP^{H})_3Bn$ determined by SC-XRD. A wagging disorder of one $[^{H}PMP^{H}]^-$ ligand was modeled.

Table S1. Crystallographic data for $Zr(^{H}PMP^{H})_3Bn$ and $Zr(^{H}PMP^{H})_4$.

	$Zr(^{H}PMP^{H})_3Bn$	$Zr(^{H}PMP^{H})_4$
chem. formula	$C_{34}H_{28}N_6Zr$	$C_{36}H_{28}N_8Zr$
cryst size, mm	0.264 × 0.245 × 0.058	0.138 x 0.226 x 0.478
Fw, g mol^{-1}	611.84	663.88
space group	P $2_1/c$	C 2/c
a, Å	14.9235(18)	16.8714(10)
b, Å	14.2433(16)	10.2281(6)
c, Å	14.793(2)	17.3048(11)
α, deg	90	90
β, deg	90.565(5)	105.228(2)
γ, deg	90	90
V, $Å^3$	3144.3(7)	2881.3(3)
Z	4	4
T, K	100(2)	100(2)
ρ calcd, g cm^{-3}	1.293	1.530
reflns collected/$2\Theta_{max}$	30538/55.626	37805/70.14
unique reflns/I > 2σ(*I*)	7289/4482	6356/5707
No. of params/restraints	470/672	204/0
λ, Å	0.71073	0.71073
R_1[a]/goodness of fit[b]	0.0589/1.027	0.0285/1.087
wR_2[c] (*I* > 2σ(*I*))	0.1139	0.0672
Residual density, $e^-/Å^{-3}$	1.04/-0.92	0.564/-0.532

[a]Observation criterion: *I* > 2σ(*I*), $R_1 = \sum((||F_O| - |F_C||) / \sum|F_O|$. [b]GoF = $[\sum[w(F_o^2 - F_c^2)^2] / (n-p)]^{1/2}$. [c]$wR_2 = [\sum[w(F_o^2 - F_c^2)^2] / \sum[w(F_o^2)^2]]^{1/2}$

5. NMR Characterization

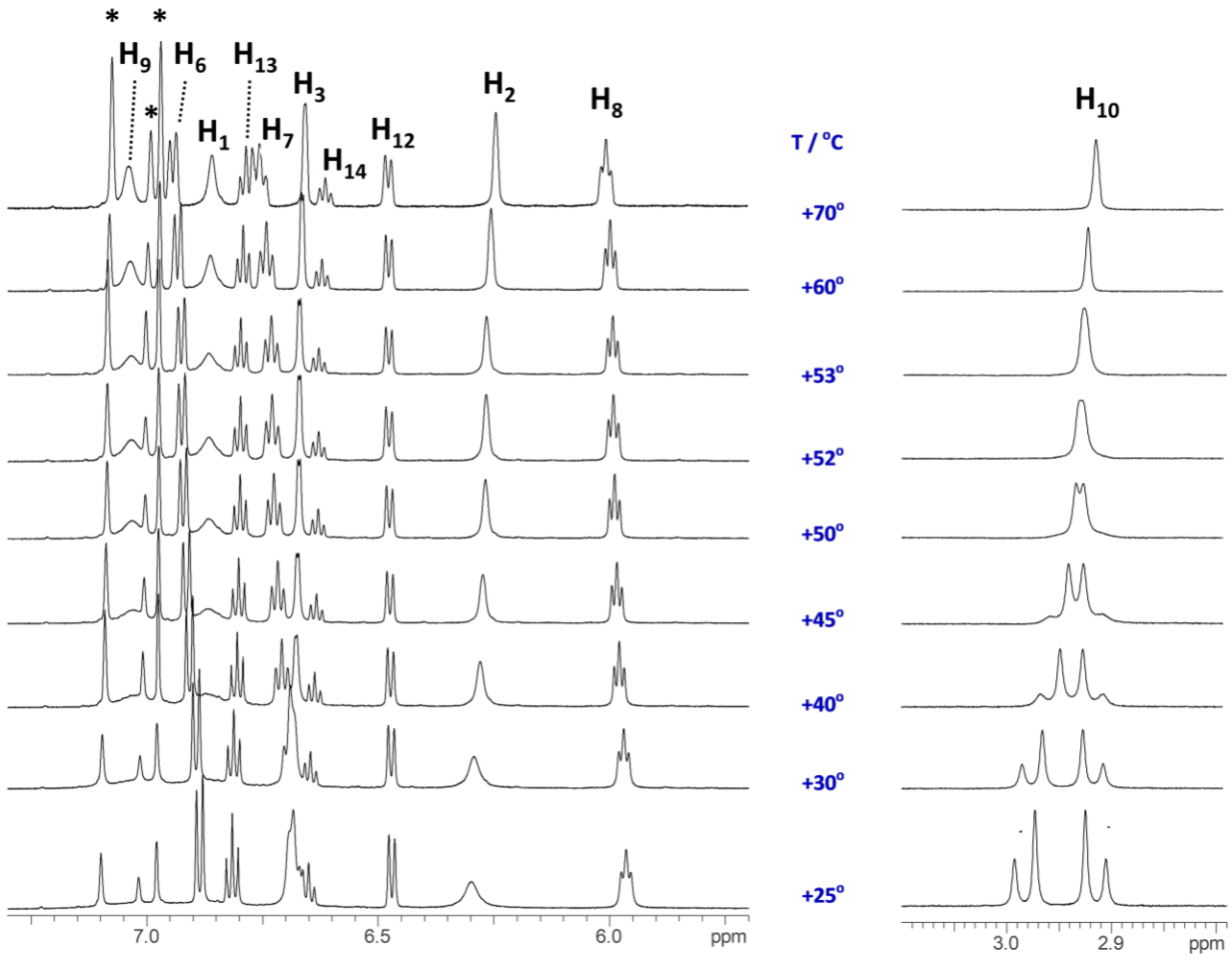

Figure S2. Variable temperature (25 °C – 70 °C) ^{1}H NMR spectra of Zr(^{H}PMP^{H})$_3$Bn recorded at 600 MHz in toluene-d_8. Assignments are based on a holistic analysis of all NMR data. Signals labelled with asterisks are from toluene-d_8.

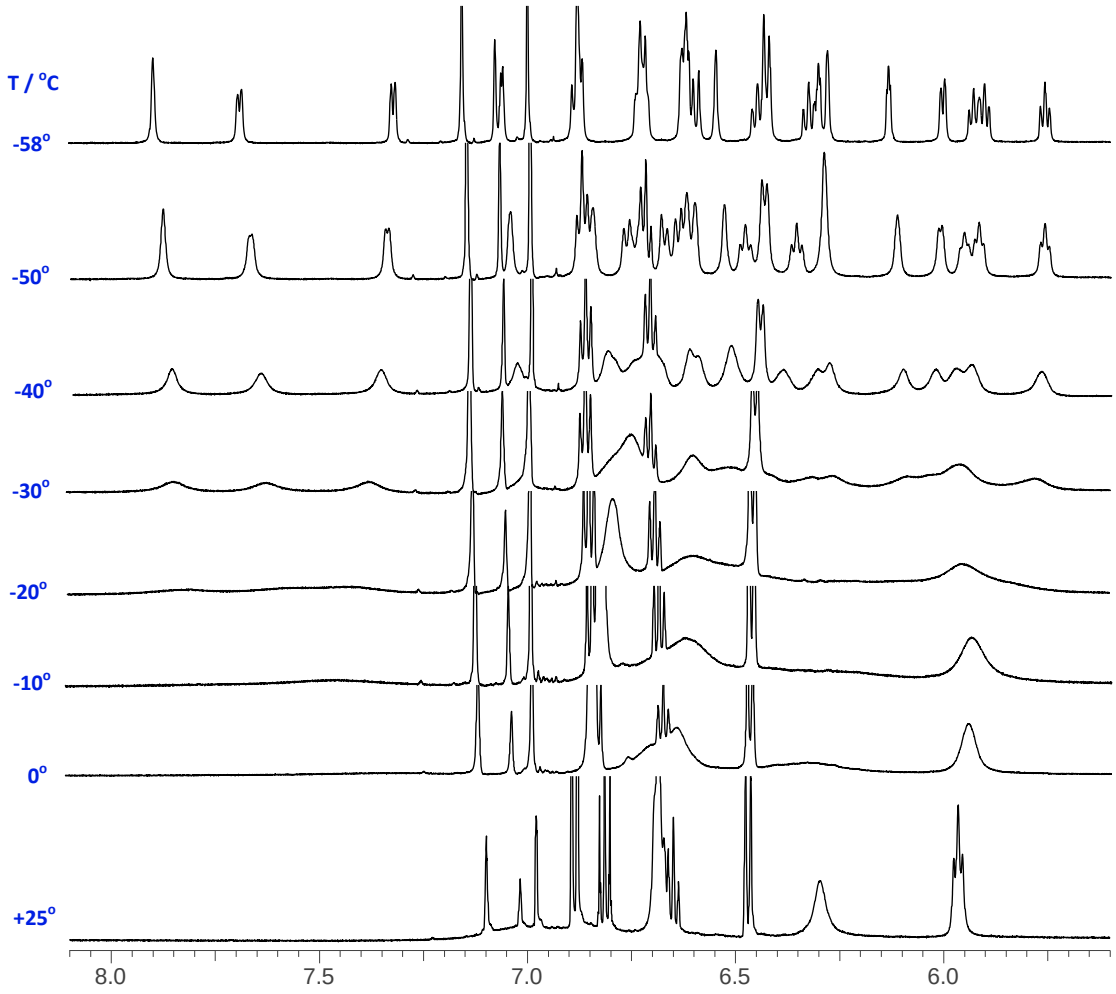

Figure S3. Variable temperature (25 °C – -58 °C) ^{1}H NMR spectra of Zr(^{H}PMP^{H})$_3$Bn recorded at 600 MHz in toluene-d_8.

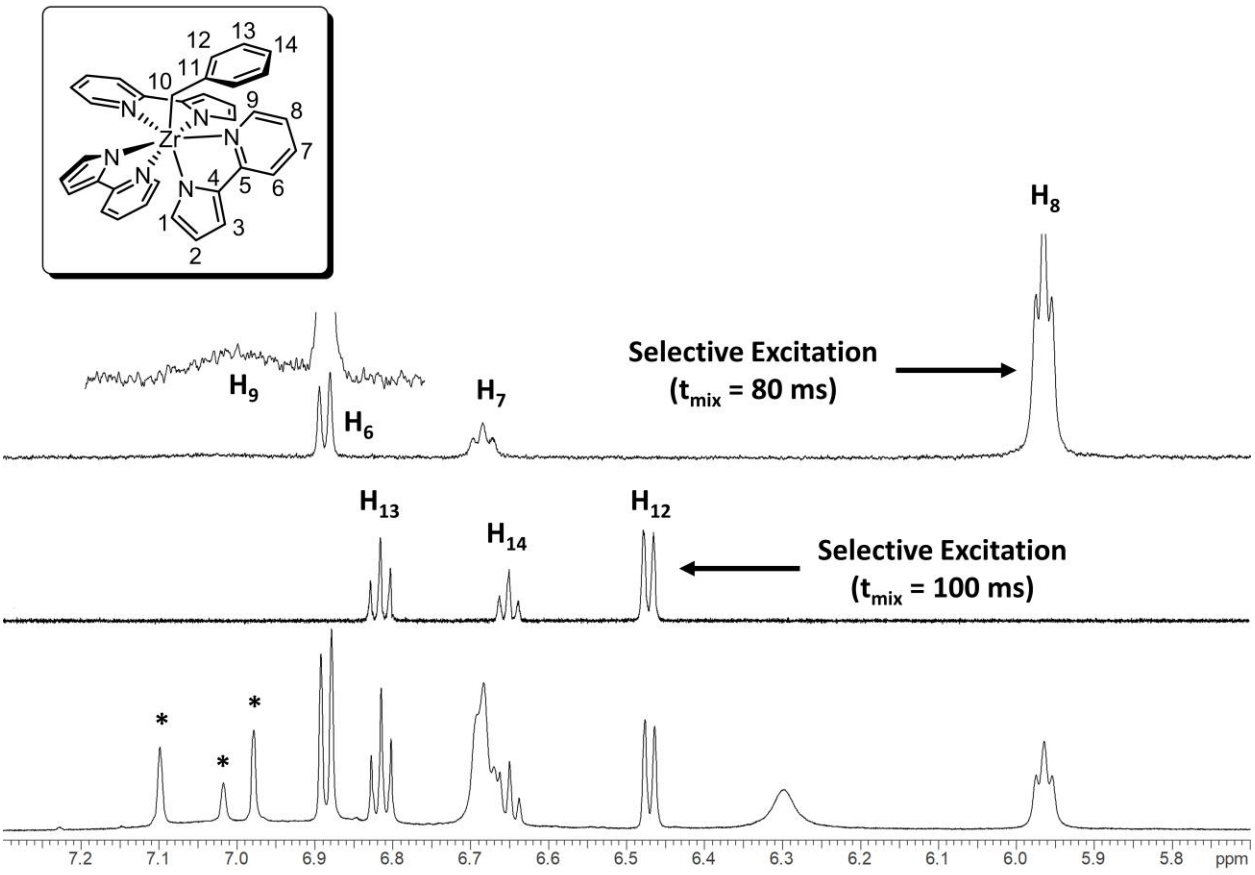

Figure S4. zTOCSY1D NMR spectra of Zr(^{H}PMP^{H})$_3$Bn recorded at 600 MHz in 25 °C toluene-d_8. The top and middle spectra represent selective excitations of the indicated signals. The normal ^{1}H NMR spectrum in toluene-d_8 is shown at the bottom to aid the reader. Assignments are based on a holistic analysis of all NMR data. Signals labelled with asterisks are from toluene-d_8.

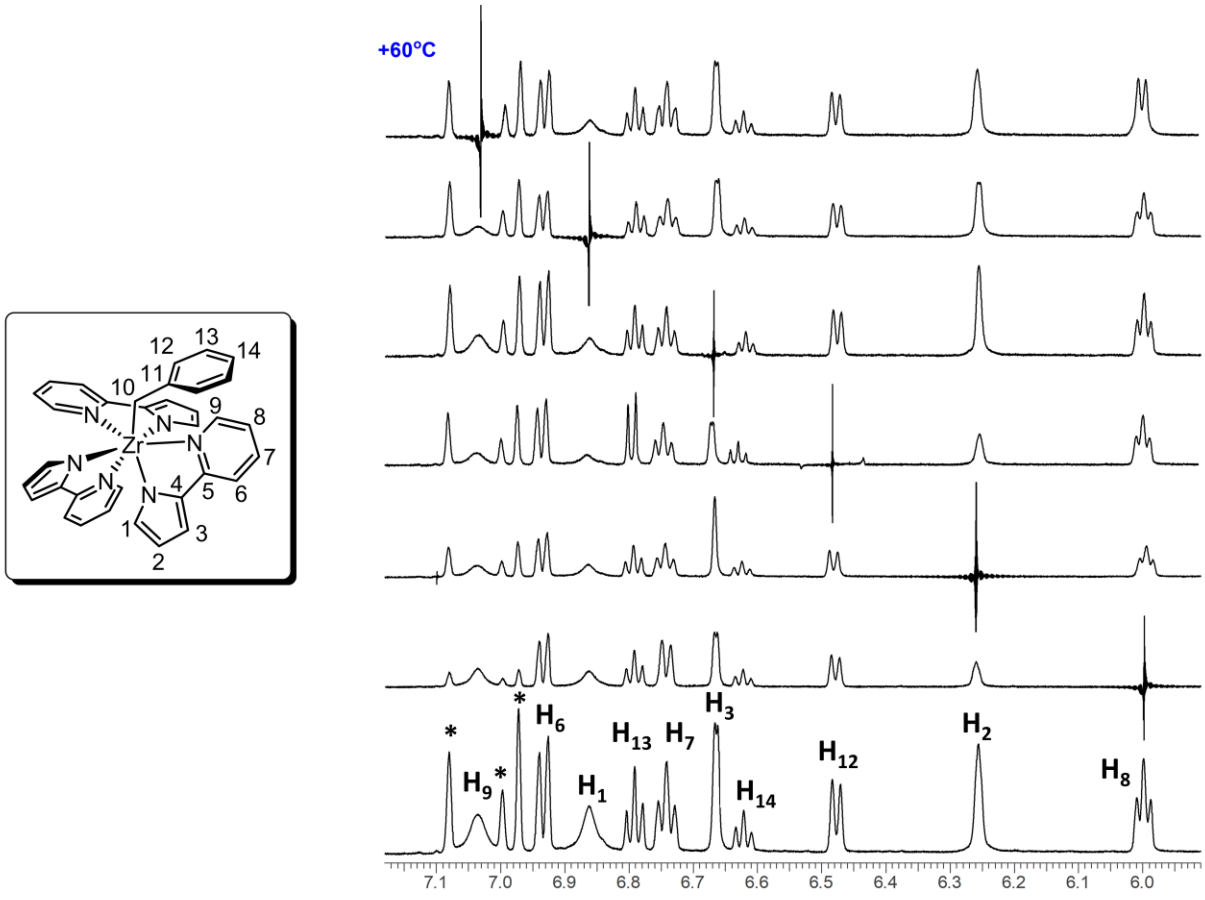

Figure S5. Selectively decoupled ^{1}H NMR spectra of Zr(^{H}PMP^{H})$_3$Bn recorded at 600 MHz in 60 °C toluene-d_8. The fully coupled ^{1}H NMR spectrum is provided at the bottom for comparison. Assignments are based on a holistic analysis of all NMR data. Signals labelled with asterisks are from toluene-d_8.

+25°C

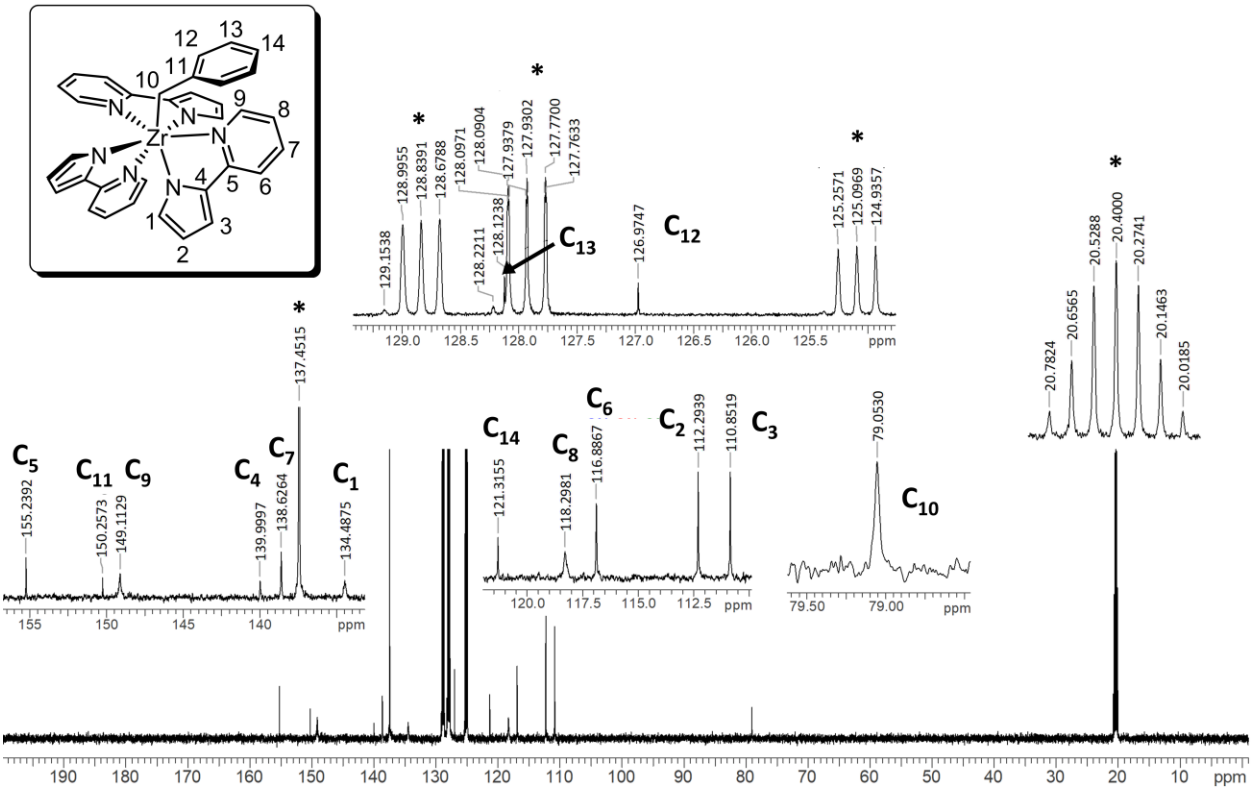

Figure S6. $^{13}C\{^{1}H\}$ NMR spectrum of Zr(^{H}PMP^{H})$_3$Bn recorded at 151 MHz in 25 °C toluene-d_8. Assignments are made on zoomed-in regions for clarity and are based on a holistic analysis of all NMR data. Signals labelled with asterisks are from toluene-d_8.

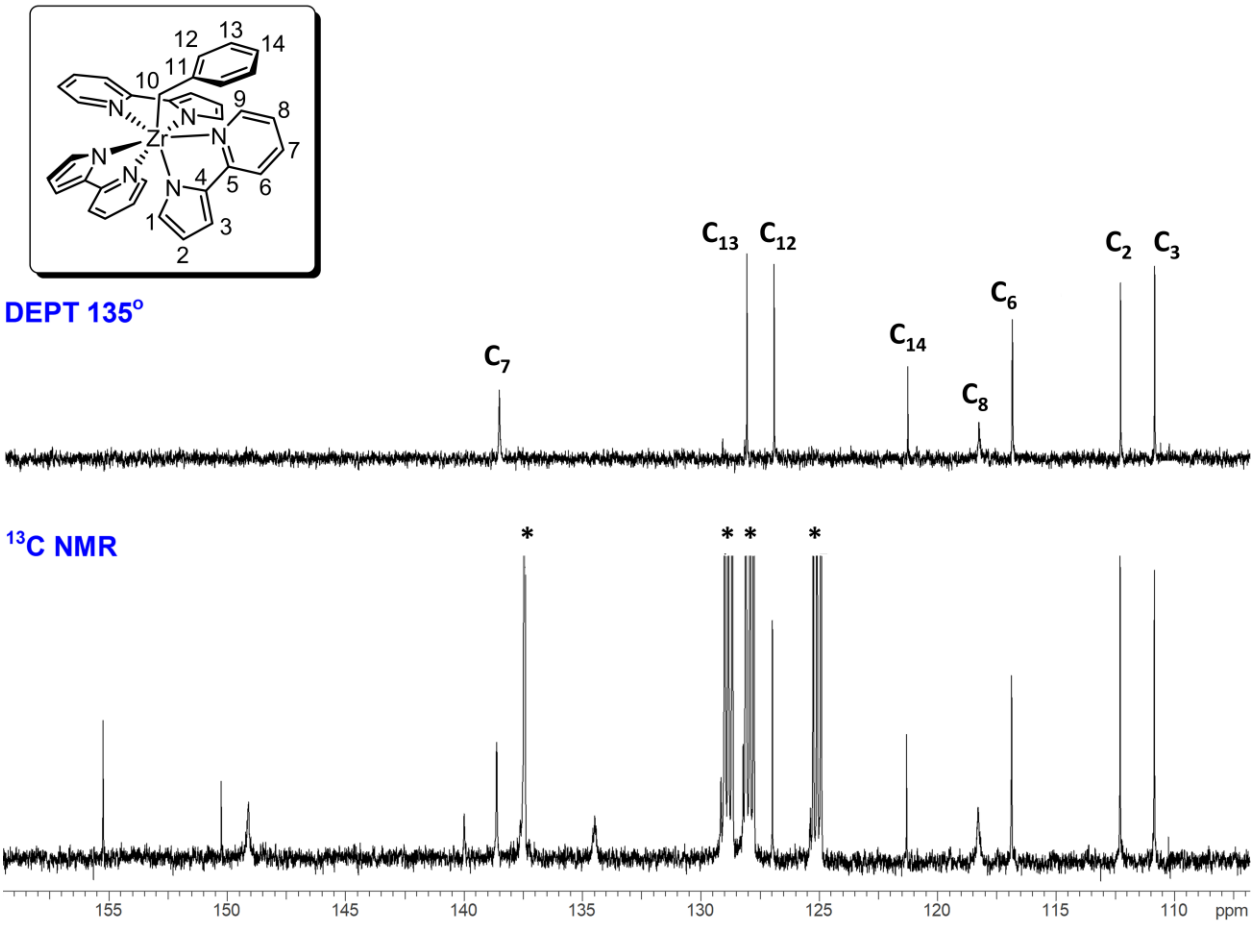

Figure S7. DEPT-135 NMR spectrum of Zr(^{H}PMP^{H})$_3$Bn recorded at 151 MHz in 25 °C toluene-d_8. Signals labelled with asterisks are from toluene-d_8. Interestingly, signals assignable to C_1 and C_9 are unobservable in the DEPT-135 spectrum but are present in all other analysis. Assignments are based on a holistic analysis of all NMR data.

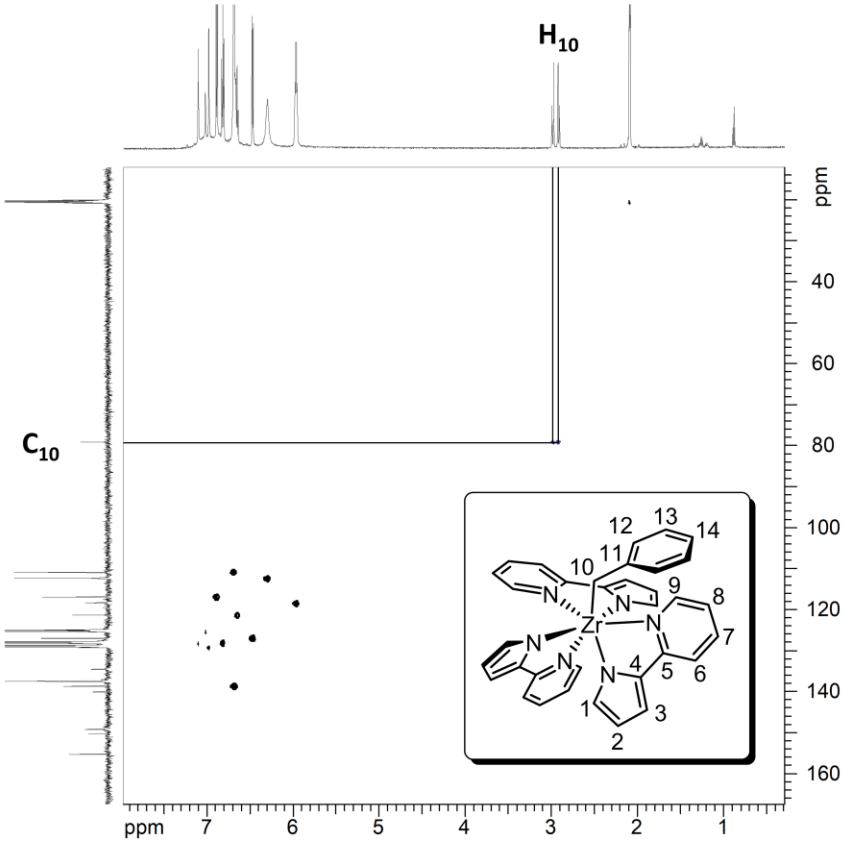

Figure S8. gHSQCAD NMR spectrum of Zr(^{H}PMP^{H})$_3$Bn recorded at 600 MHZ (^{1}H) and 151 MHz (^{13}C) in 25 °C toluene-d_8. The cross peaks between H_{10} and C_{10} are connected with lines for clarity. Assignments are based on a holistic analysis of all NMR data.

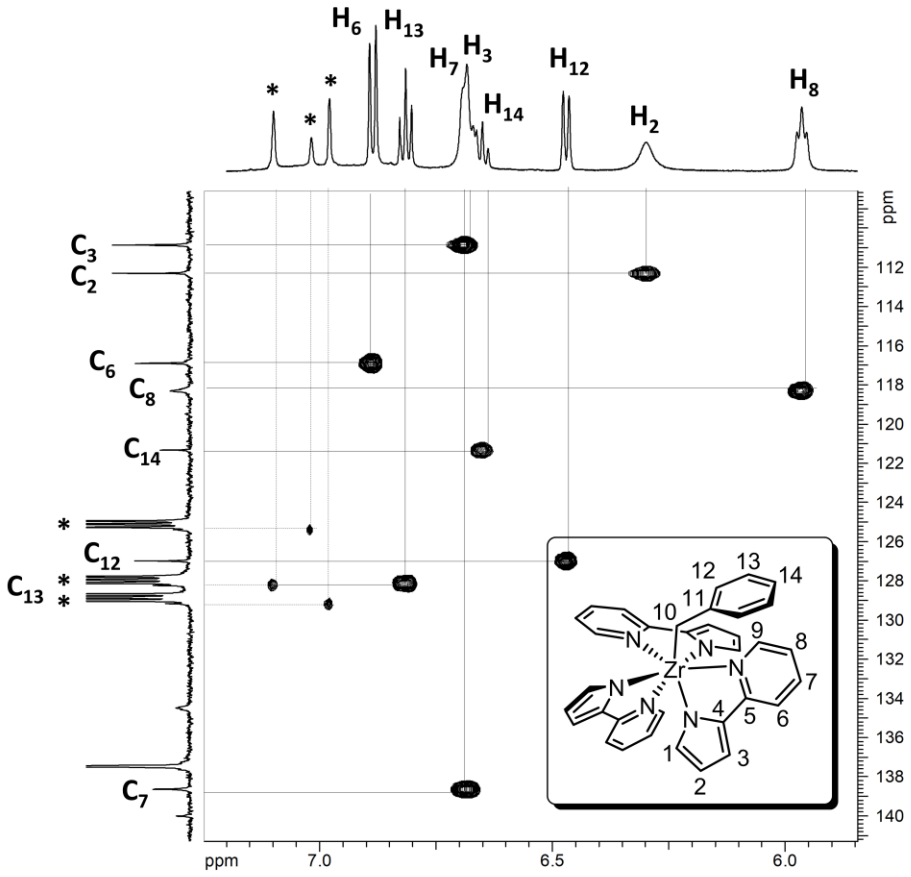

Figure S9. Expanded region of the gHSQCAD NMR spectrum of Zr(^{H}PMP^{H})$_3$Bn recorded at 600 MHZ (^{1}H) and 151 MHz (^{13}C) in 25 °C toluene-d_8. The signals are labelled and connected to cross peaks with lines for clarity. H_1 and H_9 are too broad to observe at 25 °C. Signals labelled with asterisks are from toluene-d_8. Assignments are based on a holistic analysis of all NMR data.

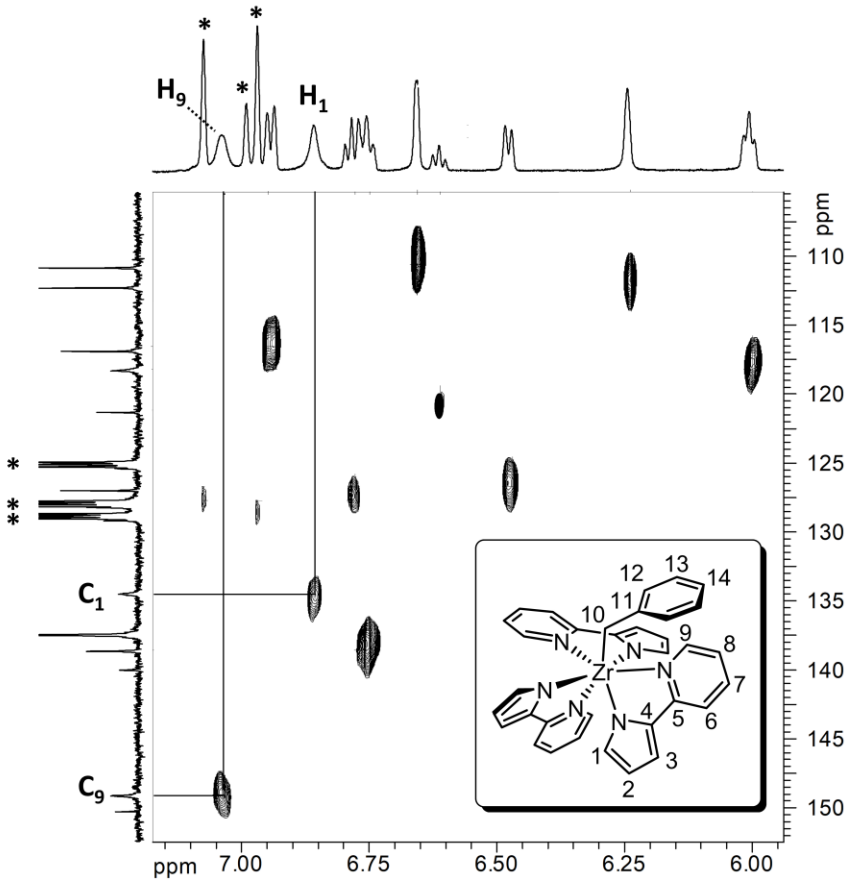

Figure S10. Expanded region of the gHSQCAD NMR spectrum of Zr(^{H}PMP^{H})$_3$Bn recorded at 600 MHZ (^{1}H) and 151 MHz (^{13}C) in 70 °C toluene-d_8. Only the signals corresponding to H_1, H_9, C_1, and C_9 are labelled and connected to their corresponding cross peaks. Signals labelled with asterisks are from toluene-d_8. Assignments are based on a holistic analysis of all NMR data.

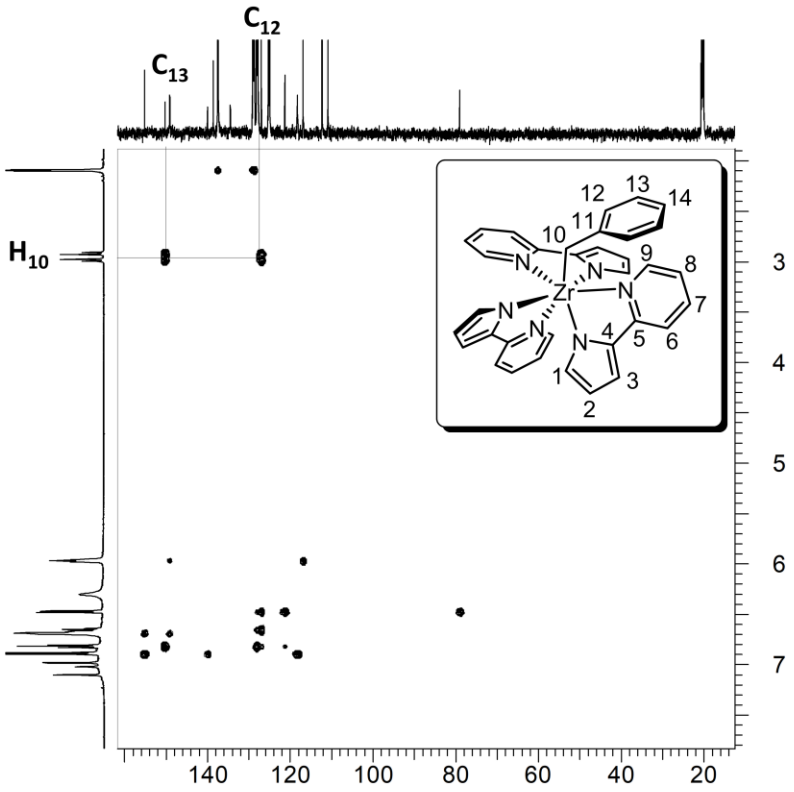

Figure S11. gHMBCAD NMR spectrum of Zr(^{H}PMP^{H})$_3$Bn recorded at 600 MHZ (^{1}H) and 151 MHz (^{13}C) in 25 °C toluene-d_8. The cross peaks for H_{10} are connected to the corresponding signals with lines. Assignments are based on a holistic analysis of all NMR data.

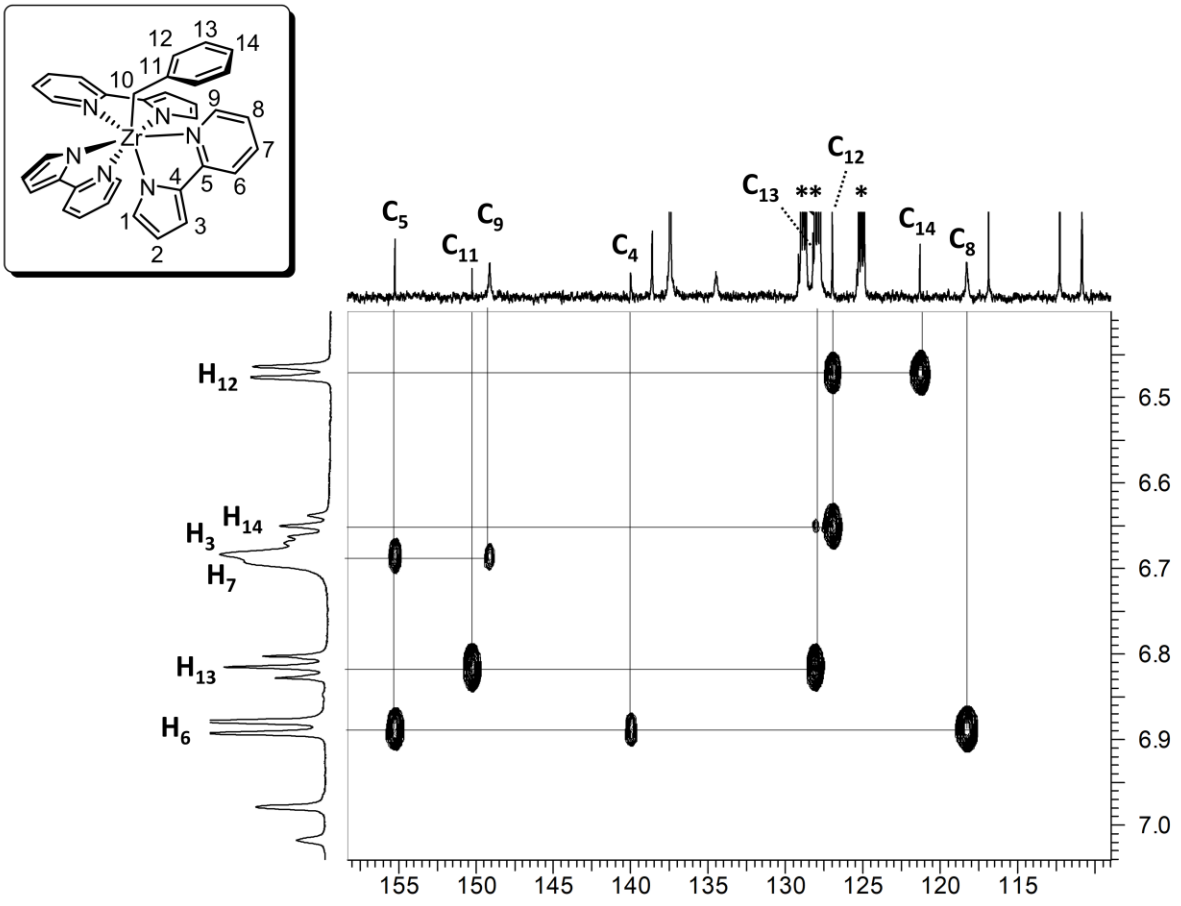

Figure S12. Expanded region of the gHMBCAD NMR spectrum of Zr(^{H}PMP^{H})$_3$Bn recorded at 600 MHZ (^{1}H) and 151 MHz (^{13}C) in 25 °C toluene-d_8. The signals are labelled and connected to cross peaks with lines for clarity. Signals labelled with asterisks are from toluene-d_8. Assignments are based on a holistic analysis of all NMR data.

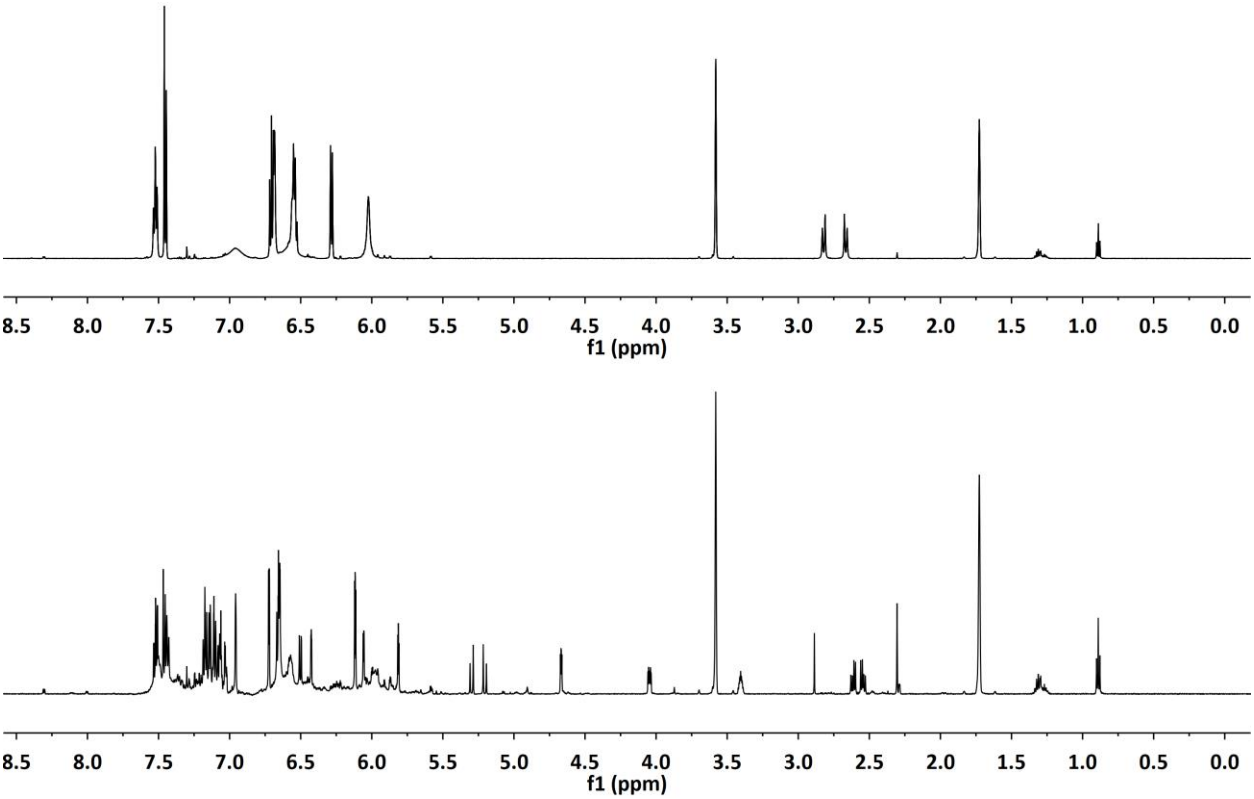

Figure S13. 600 MHz ^{1}H NMR spectrum of Zr(^{H}PMP^{H})$_3$Bn collected in 25 °C thf-d_8 after: [top] 0 minutes of exposure to ambient light; [bottom] several hours of exposure to ambient light.

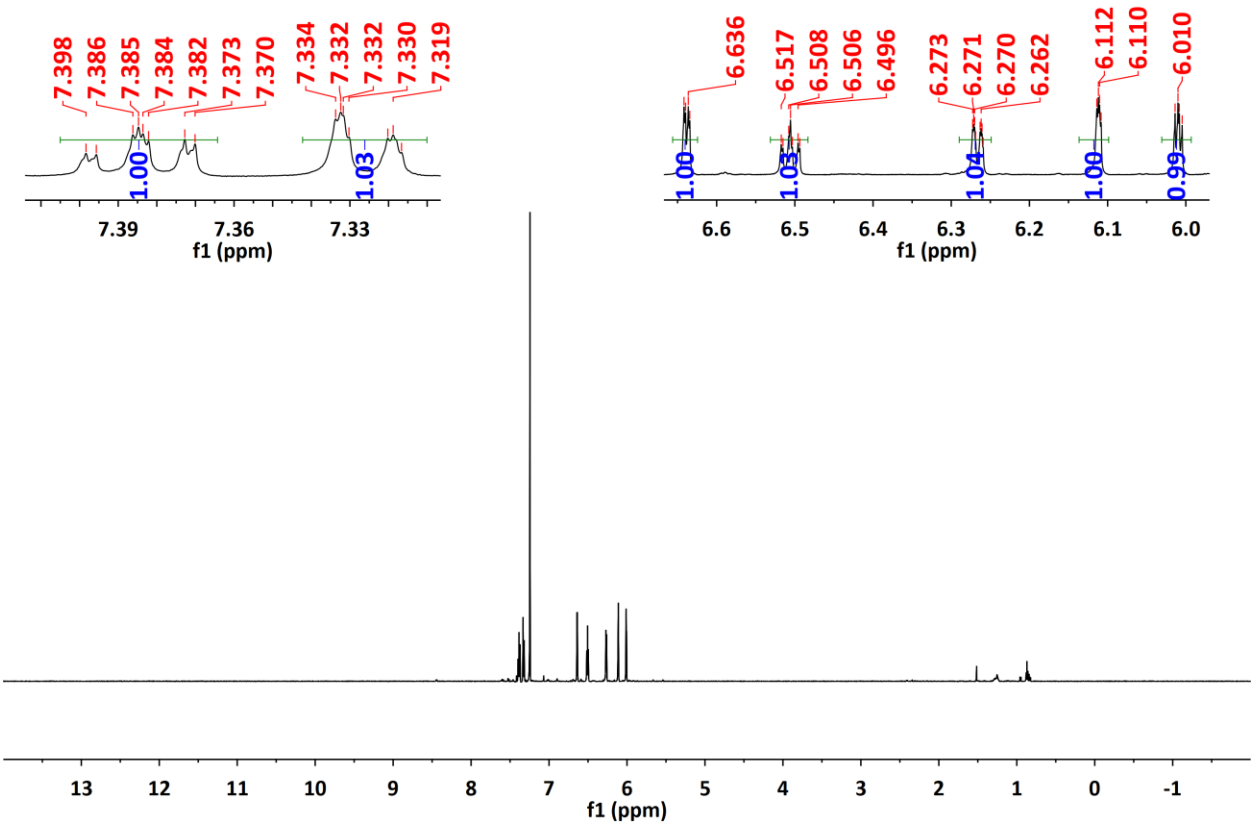

Figure S14. 600 MHz ^{1}H NMR spectrum of Zr(^{H}PMP^{H})$_4$ collected in 25 °C $CDCl_3$.

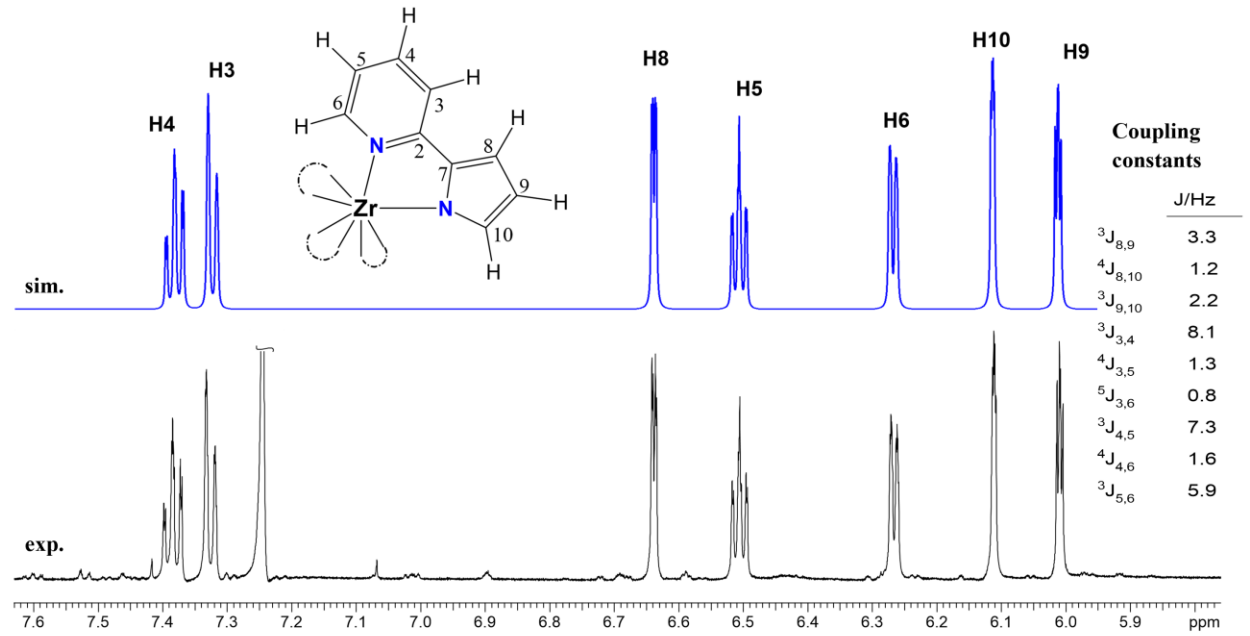

Figure S15. Experimental (bottom) and calculated (top) ^{1}H NMR spectrum of Zr(^{H}PMP^{H})$_4$ in $CDCl_3$.

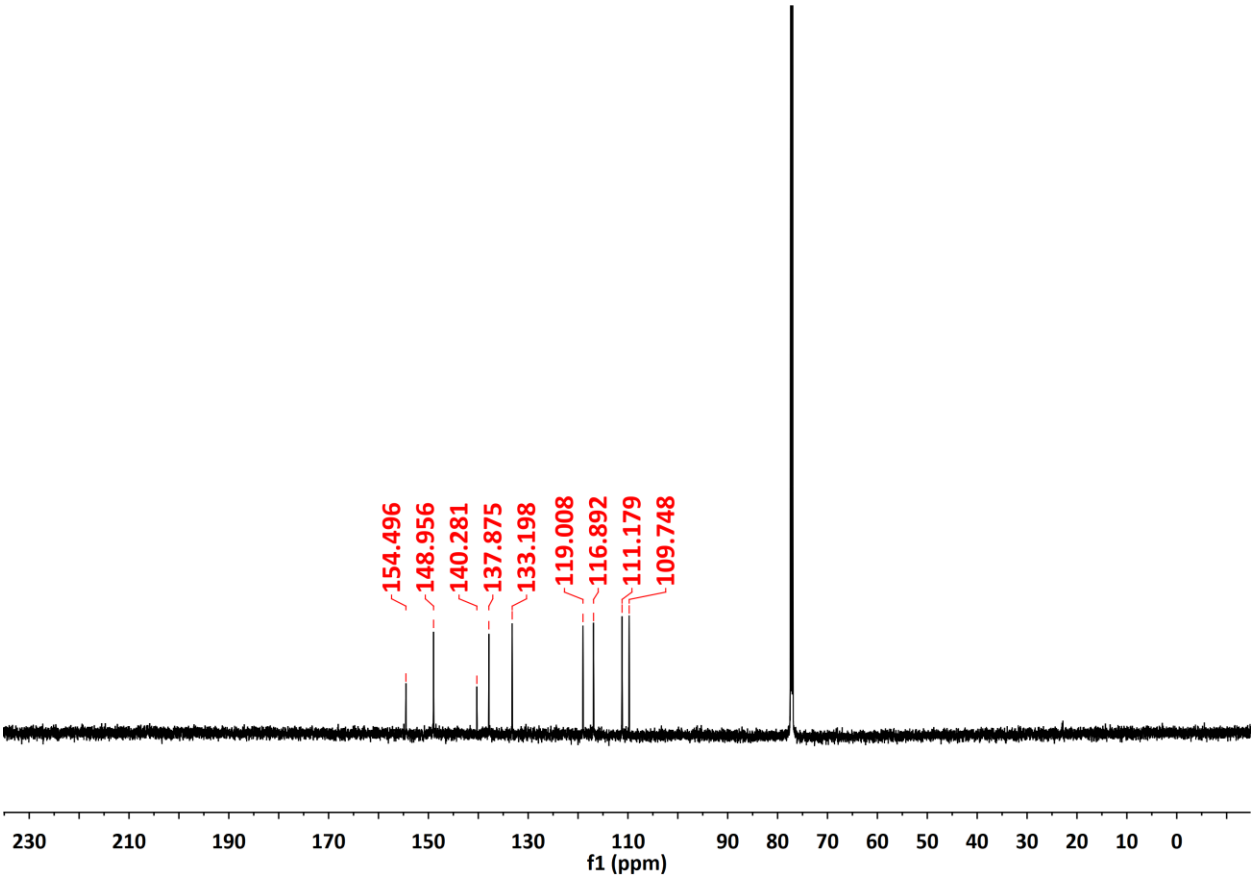

Figure S16. 151 MHz $^{13}C\{^{1}H\}$ NMR spectrum of $Zr(^{H}PMP^{H})_4$ collected in 25 °C $CDCl_3$.

6. Photophysical Measurements

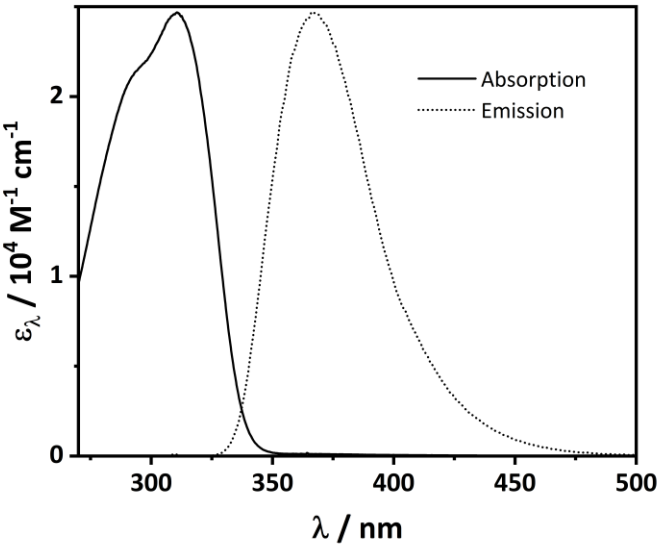

Figure S17. Absorption (solid) and normalized emission (dotted) spectra of the free ligand $H^{H}PMP^{H}$ obtained in dichloromethane solution. The emission spectrum was recorded after excitation of the band centered at 310 nm.

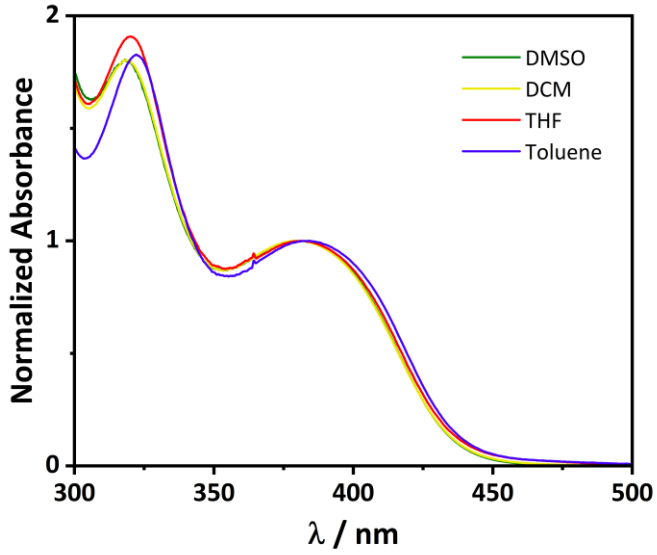

Figure S18. Normalized absorption spectra of $Zr(^{H}PMP^{H})_4$ in varying solvents. A light source switch causes minor scattering at 355 nm.

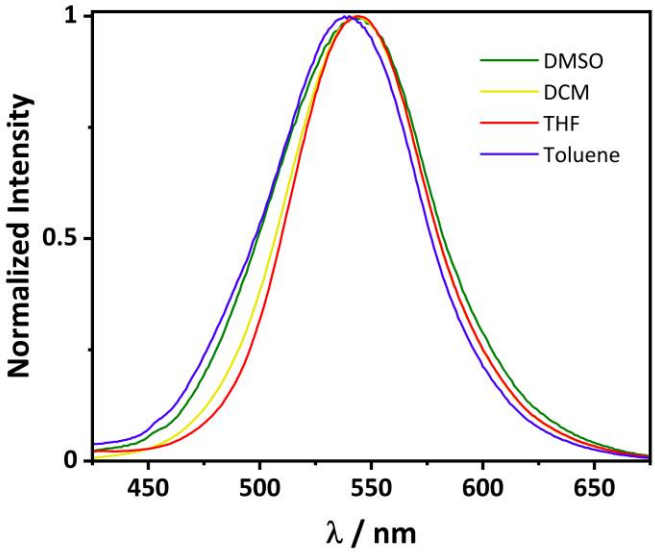

Figure S19. Normalized emission spectra (λ_{exc} = 400 nm) of Zr(^{H}PMP^{H})$_4$ in varying solvents.

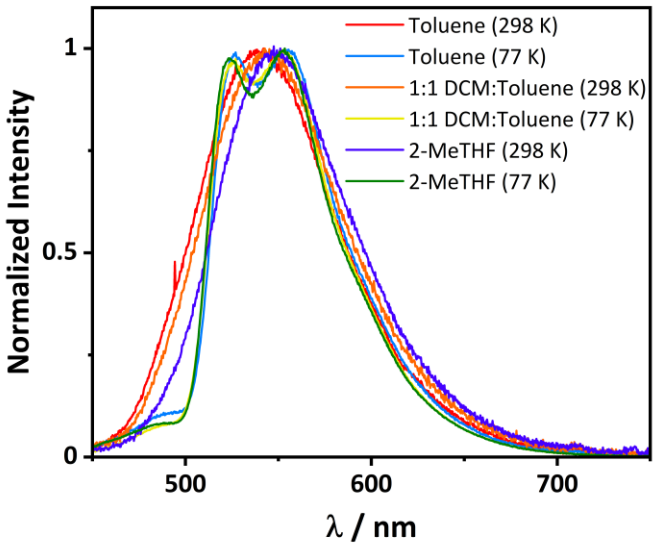

Figure S20. Emission spectra (λ_{exc} = 370 nm) collected at room temperature and at 77 K in frozen solution. Additional features assigned as vibrational fine structure are observed in all solvents when cooled to 77 K.

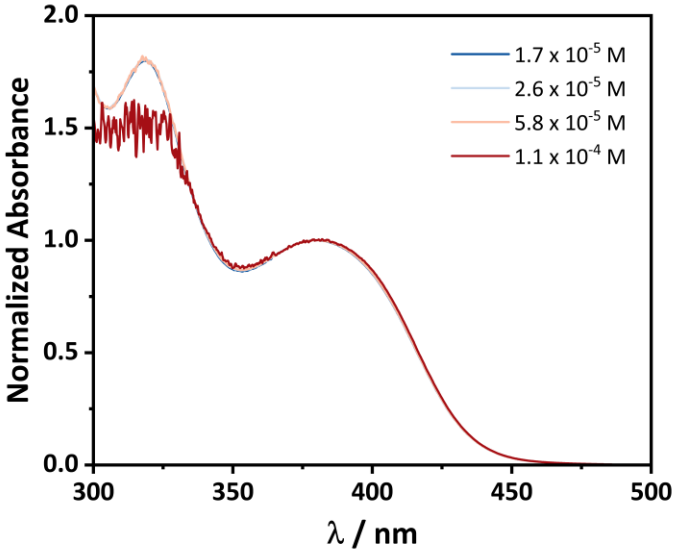

Figure S21. Normalized absorption spectra collected at variable concentrations. Solutions more concentrated than *ca.* 1.1 x 10^{-4} M were found to absorb too strongly for a meaningful absorption profile comparison.

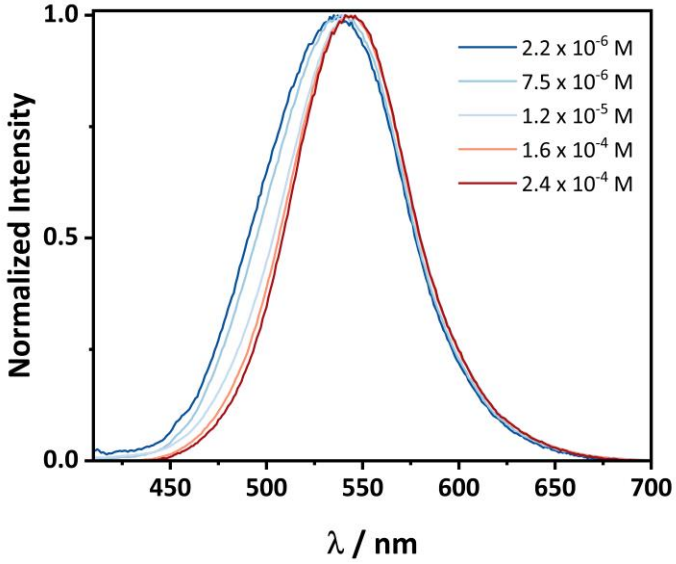

Figure S22. Emission spectra (λ_{exc} = 400 nm) collected at variable concentrations.

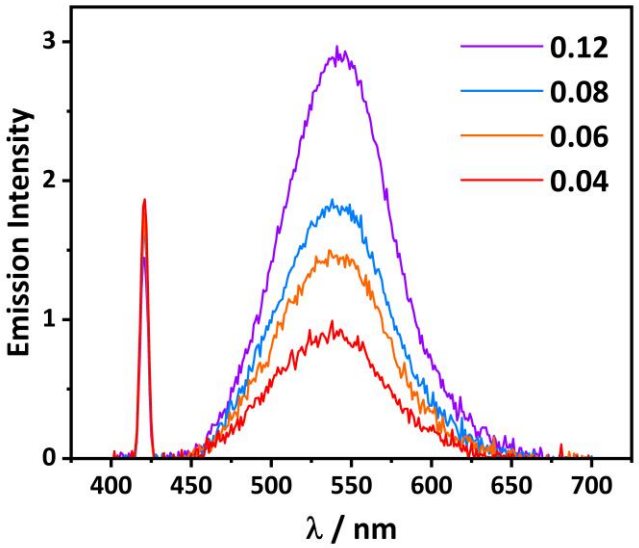

Figure S23. Emission spectra (λ_{exc} = 422 nm) collected (at *ca.* 0.04-0.12 absorbance) during photoluminescence quantum yield determination.

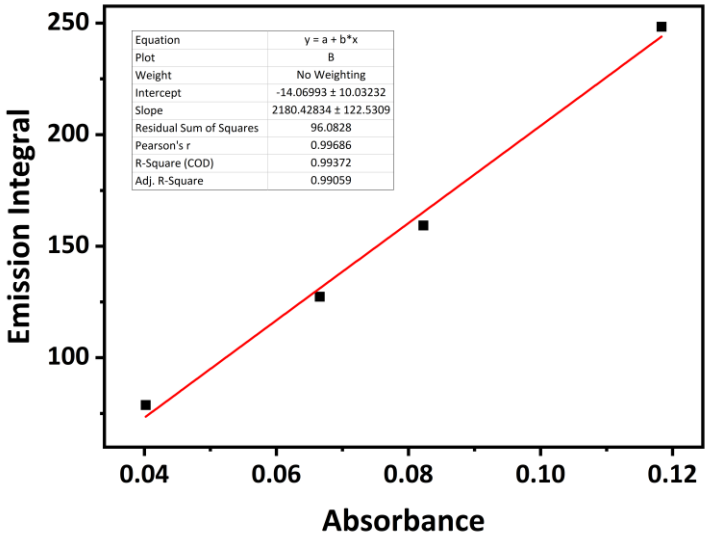

Figure S24. Fit of quantum yield determination data. The quantum yield was determined *via* the comparative method using coumarin-153 (Φ_{422nm} = 0.53 in ethanol)[3] as the standard.

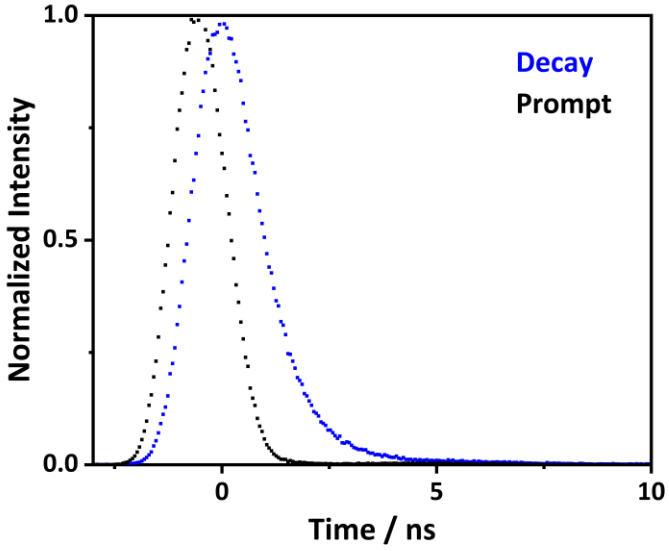

Figure S25. Luminescence decay of $Zr(HPMPH)_4$ recorded in DCM solution under ambient atmospheric conditions.

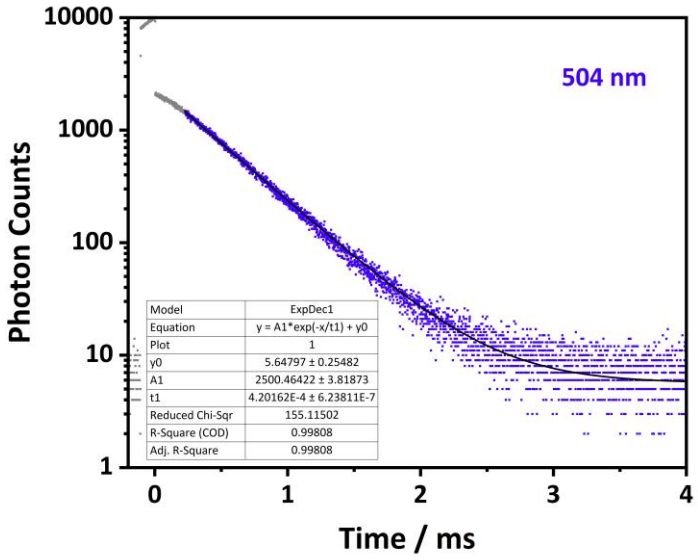

Figure S26. Manual fit of the luminescence decay monitored at 504 nm. The data was fit (black line) excluding the initial nonlinear region shown in grey.

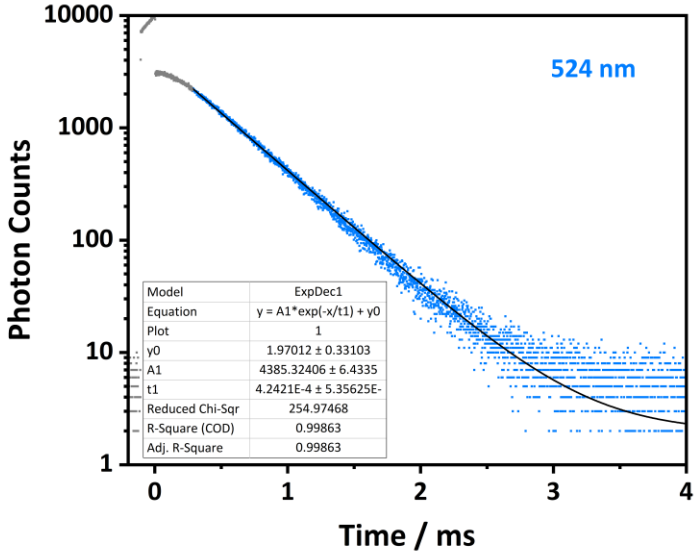

Figure S27. Manual fit of the luminescence decay monitored at 524 nm. The data was fit (black line) excluding the initial nonlinear region shown in grey.

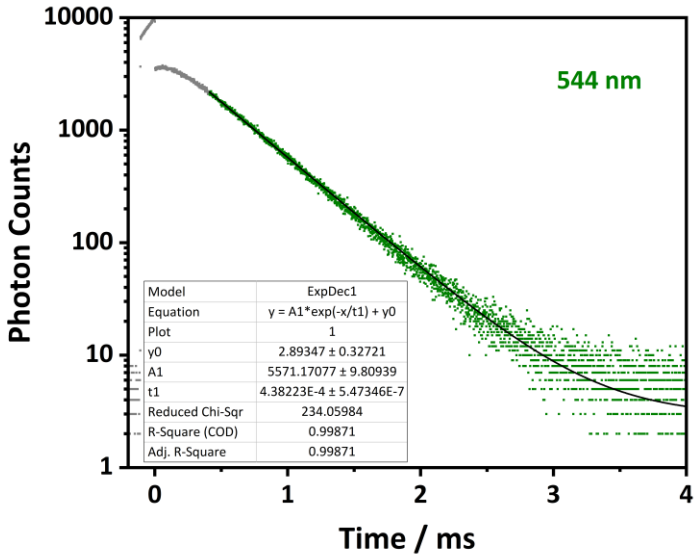

Figure S28. Manual fit of the luminescence decay monitored at 544 nm. The data was fit (black line) excluding the initial nonlinear region shown in grey.

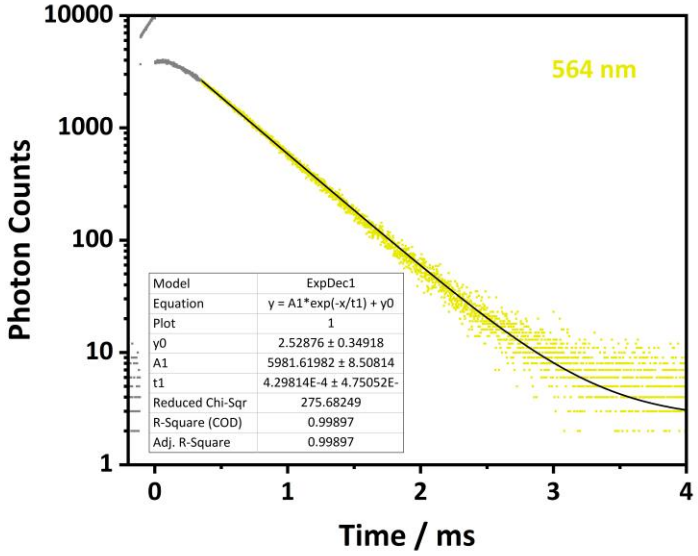

Figure S29. Manual fit of the luminescence decay monitored at 564 nm. The data was fit (black line) excluding the initial nonlinear region shown in grey.

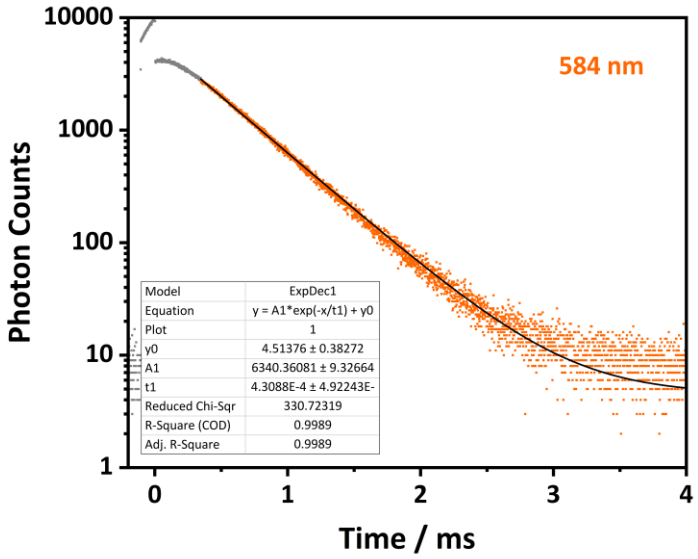

Figure S30. Manual fit of the luminescence decay monitored at 584 nm. The data was fit (black line) excluding the initial nonlinear region shown in grey.

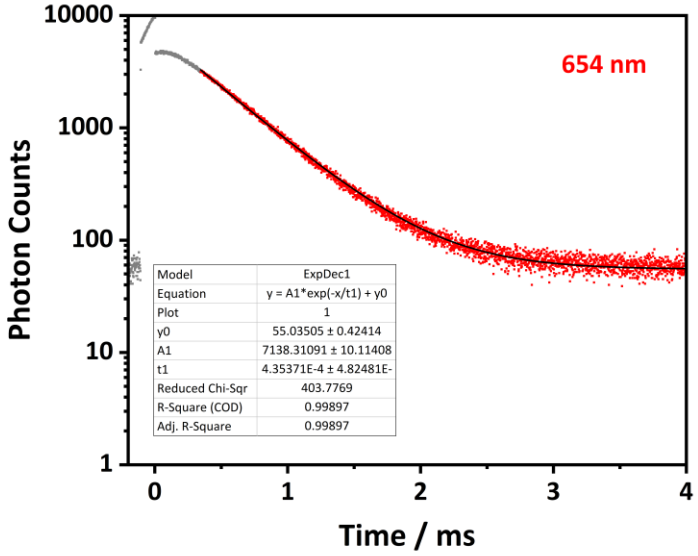

Figure S31. Manual fit of the luminescence decay monitored at 654 nm. The data was fit (black line) excluding the initial nonlinear region shown in grey.

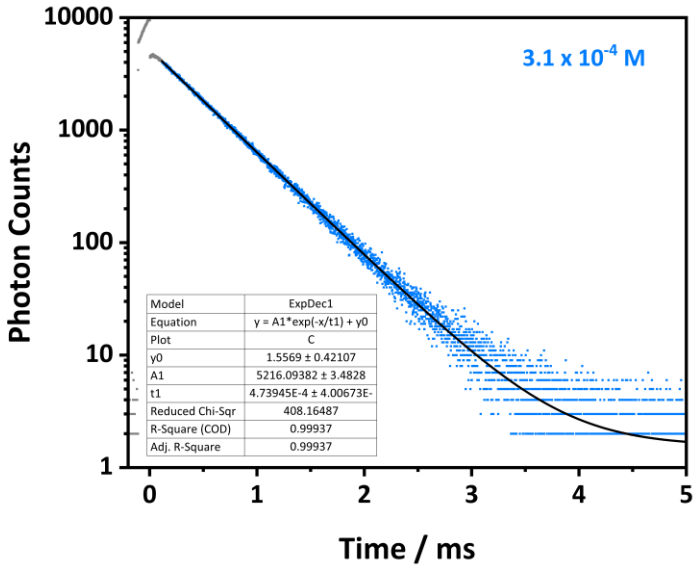

Figure S32. Manual fit of the luminescence decay monitored at 544 nm with a concentration of 3.1 x 10^{-4} M. The data was fit (black line) excluding the initial nonlinear region shown in grey.

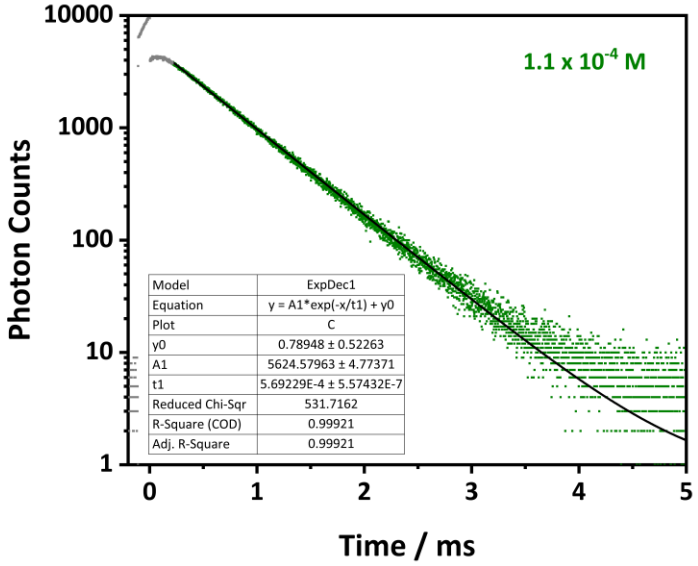

Figure S 33. Manual fit of the luminescence decay monitored at 544 nm with a concentration of 1.1 x 10^{-4} M. The data was fit (black line) excluding the initial nonlinear region shown in grey.

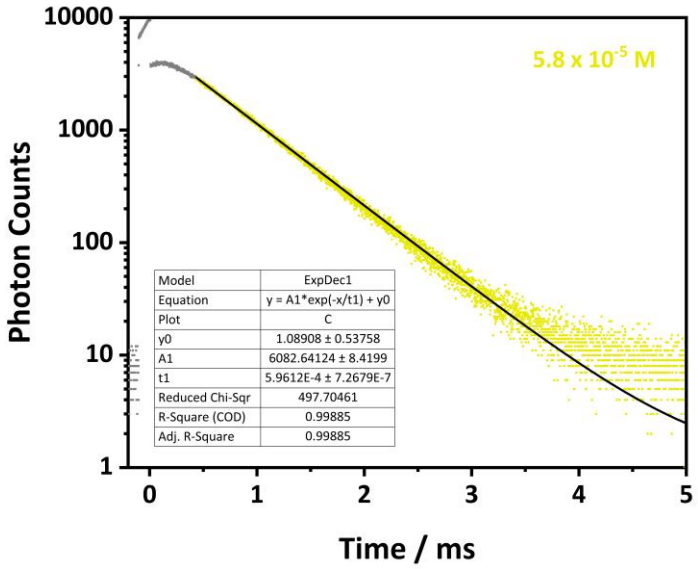

Figure S34. Manual fit of the luminescence decay monitored at 544 nm with a concentration of 5.8 x 10^{-5} M. The data was fit (black line) excluding the initial nonlinear region shown in grey.

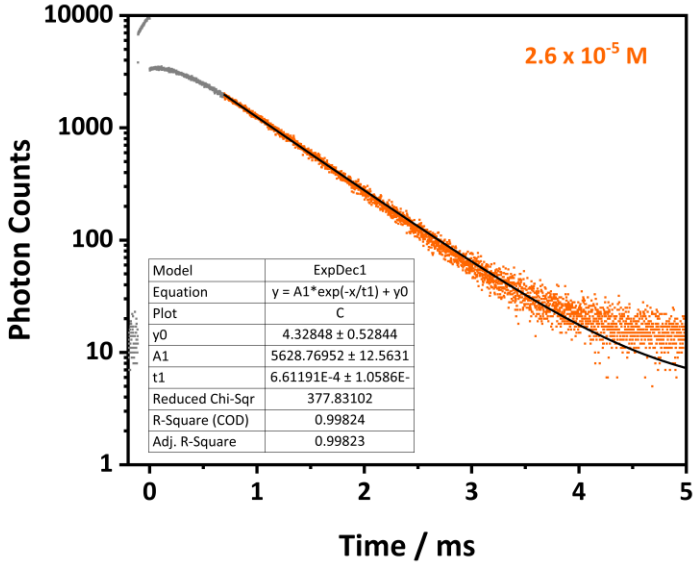

Figure S35. Manual fit of the luminescence decay monitored at 544 nm with a concentration of 2.6 x 10^{-5} M. The data was fit (black line) excluding the initial nonlinear region shown in grey.

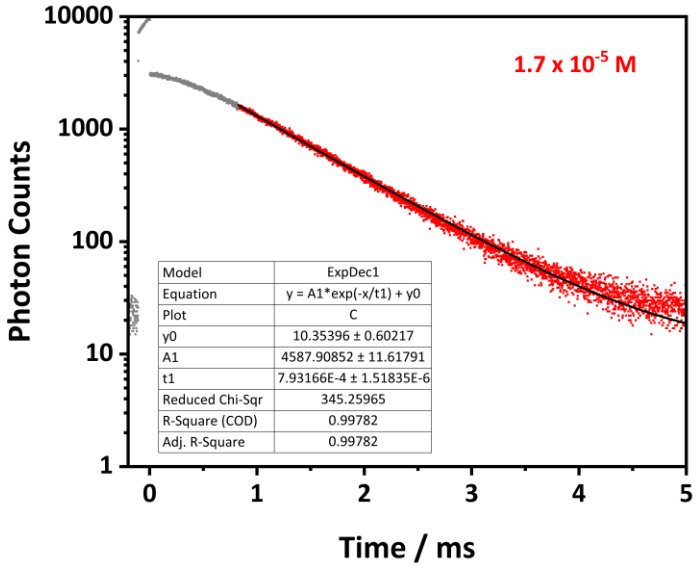

Figure S 36. Manual fit of the luminescence decay monitored at 544 nm with a concentration of 1.7 x 10^{-5} M. The data was fit (black line) excluding the initial nonlinear region shown in grey.

7. Computational Details

All calculations were performed using the ORCA quantum chemical program package v5.0.1.[4,5] Geometry optimizations and TD-DFT calculations used the B3LYP density functional.[6] In all cases, scalar-relativistic effects were included *via* the zeroth-order regular approximation (ZORA).[7] The relativistically recontracted triple-ζ quality basis set, ZORA-def2-TZVP,[8] was used for nitrogen atoms while the SARC-ZORA-TZVP[9] was used for zirconium. All other atoms were handled with the recontracted split-valence ZORA-def2-SVP basis set.[8] The calculations were accelerated using the RIJCOSX approximation[10,11] in tandem with the decontracted SARC/J auxiliary basis set. In geometry optimizations, noncovalent interactions were considered *via* atom-pairwise dispersion corrections with Becke–Johnson (D3BJ) damping.[12,13] All solvation effects resulting from dichloromethane were handled using the conductor-like polarizable continuum model (C-PCM) and a gaussian charge scheme.[14] All structural and density plots were made using Chemcraft.[15]

7.1 Input Files and Coordinates

Geometry Optimization and Frequency Calculation

```
!rks b3lyp d3bj tightscf zora zora-def2-svp sarc/j normalprint tightopt cpcm(ch2cl2) numfreq
%pal nprocs 40 end
%maxcore 2000
%basis newgto Zr "sarc-zora-tzvp" end
    newgto N "zora-def2-tzvp" end
 end
*xyz 0 1
```

TD-DFT Calculation

```
!rks b3lyp tightscf zora zora-def2-svp sarc/j normalprint printmos printbasis cpcm(ch2cl2)
%pal nprocs 20 end
%maxcore 4000
%basis newgto Zr "sarc-zora-tzvp" end
    newgto N "zora-def2-tzvp" end
end
%tddft nroots 50
    donto true
    ntostates 1,2,3,4,5,6,7,8,9,10
    tda false
    upop true
    triplets true
    irootlist 1,2,3,4,5,6,7,8,9,10
    trootlist 1,2,3,4,5,6,7,8,9,10
end
*xyz 0 1
```

Optimized S_0 Coordinates

Zr	-0.00000123112115	-0.00000154779252	0.00001425036517
N	1.25803559637005	-1.70460798977700	-0.75157313555054
N	0.67022342277620	-1.21765738109009	1.98414533454711
N	-1.70475454239438	-1.25786020880916	0.75158051576920
N	1.21755890324242	0.67038553017023	-1.98413126872580
N	-1.25804035114531	1.70460248110313	-0.75157018774390
N	-0.67022481417664	1.21766043526919	1.98414279530511
N	1.70475282821890	1.25786139224554	0.75157382296147
N	-1.21756144002067	-0.67038834492903	-1.98413430715100
C	-0.31381823065630	-1.89045671347144	2.63142002628382
C	-3.01392552350178	-1.34256978689081	0.37248604726048
H	-3.35115057315738	-0.92408581579272	-0.56807156637232
C	-2.85564754279460	-2.35648056403251	2.38295242092361
H	-3.08243302495223	-2.88854859959357	3.30190667357094
C	1.34287034107581	-3.01378101170965	-0.37250619079756
H	0.92444242917767	-3.35105675399605	0.56805813890214
C	-1.60260459986303	-1.87527289319627	1.98616730240600
C	1.87540138504492	-1.60238180852441	-1.98617860542058
C	1.89044890602393	-0.31358561985071	-2.63141894020950
C	-3.75991252021056	-2.00862468638341	1.34938321418454
H	-4.82383422272826	-2.22330597689873	1.31076714546697
C	1.91449063008781	-1.21176355985806	2.48299533345593
H	2.66216525149594	-0.67727940832333	1.90368748599122
C	2.24865367724321	-1.85049554826464	3.67072740111299
H	3.27179585870276	-1.81663787206661	4.03701378567063
C	1.21156174517356	1.91465919183120	-2.48295710481352
H	0.67701370447575	2.66228171949736	-1.90364017542934
C	2.55062601696836	-0.04896278847605	-3.84731938728347
H	3.07773087333110	-0.85214408760137	-4.35652856292075
C	2.00896734904753	-3.75968952346173	-1.34943471723070
H	2.22374761620297	-4.82359226900673	-1.31084497971291
C	2.35671232353358	-2.85537478756221	-2.38299643145880
H	2.88877531715345	-3.08209458768871	-3.30196982021736
C	-0.04927120241942	-2.55066485278899	3.84731995181311
H	-0.85250653849230	-3.07769667381863	4.35651934832965
C	1.23691416896910	-2.52560673873208	4.37028739027041
H	1.45663939510353	-3.03240060974564	5.30889057520092
C	1.85026137798679	2.24889798070491	-3.67068668957207
H	1.81631774132841	3.27204523811544	-4.03695084533460
C	2.52545216857720	1.23722782792475	-4.37026880711032
H	3.03221706438905	1.45700989368444	-5.30887447690643
C	0.31381816242724	1.89045905411995	2.63141561262400
C	3.01392474888522	1.34256731037954	0.37248119330527
H	3.35114970518866	0.92408337497487	-0.56807638673001
C	2.85564744251293	2.35647860806142	2.38294729554628
H	3.08243306903331	2.88854645911144	3.30190161181101
C	-1.34287603444656	3.01377509832066	-0.37250147527676
H	-0.92444896304661	3.35105013578246	0.56806335364078
C	1.60260375055344	1.87527401185584	1.98616103968415
C	-1.87540374991494	1.60237871370201	-1.98617719942734
C	-1.89044968444262	0.31358434769361	-2.63142104280812
C	3.75991249694818	2.00862042305301	1.34937897536321
H	4.82383472630018	2.22329941252143	1.31076371646939
C	-1.91449092887349	1.21176618367631	2.48299551939706
H	-2.66216649110614	0.67728134011786	1.90368968112652
C	-2.24865205985535	1.85049951432895	3.67072731554461
H	-3.27179369211788	1.81664211482337	4.03701524519898
C	-1.21156293755209	-1.91466071030278	-2.48296323158163
H	-0.67701609904943	-2.66228448433560	-1.90364677763209
C	-2.55062236331464	0.04896517414126	-3.84732458771428
H	-3.07772461068339	0.85214822098181	-4.35653369814215
C	-2.00897151793060	3.75968510184741	-1.34942965986024
H	-2.22375193149530	4.82358772044013	-1.31083828041774
C	-2.35671421154200	2.85537213218235	-2.38299369363954

H	-2.88877551522948	3.08209339990345	-3.30196768269168
C	0.04927309882170	2.55066942174501	3.84731481360158
H	0.85250892727943	3.07770206133504	4.35651254235391
C	-1.23691140805877	2.52561196562866	4.37028444083599
H	-1.45663511240853	3.03240719249220	5.30888726960488
C	-1.85025896795346	-2.24889618398383	-3.67069565794270
H	-1.81631390748349	-3.27204241814598	-4.03696254220790
C	-2.52544716988982	-1.23722407126303	-4.37027736799993
H	-3.03220850562169	-1.45700330560216	-5.30888560186543

S_0 Vibrational Frequencies

0: 0.00 cm**-1
1: 0.00 cm**-1
2: 0.00 cm**-1
3: 0.00 cm**-1
4: 0.00 cm**-1
5: 0.00 cm**-1
6: 27.42 cm**-1
7: 36.17 cm**-1
8: 39.03 cm**-1
9: 46.98 cm**-1
10: 47.02 cm**-1
11: 51.95 cm**-1
12: 59.88 cm**-1
13: 65.62 cm**-1
14: 65.67 cm**-1
15: 106.22 cm**-1
16: 109.25 cm**-1
17: 116.75 cm**-1
18: 116.78 cm**-1
19: 122.56 cm**-1
20: 122.58 cm**-1
21: 133.55 cm**-1
22: 152.20 cm**-1
23: 163.39 cm**-1
24: 163.40 cm**-1
25: 169.92 cm**-1
26: 181.22 cm**-1
27: 181.28 cm**-1
28: 183.77 cm**-1
29: 197.17 cm**-1
30: 214.42 cm**-1
31: 225.89 cm**-1
32: 230.50 cm**-1
33: 235.74 cm**-1
34: 235.75 cm**-1
35: 241.88 cm**-1
36: 281.21 cm**-1
37: 281.21 cm**-1
38: 294.43 cm**-1
39: 295.51 cm**-1
40: 302.05 cm**-1
41: 302.07 cm**-1
42: 303.76 cm**-1
43: 393.15 cm**-1
44: 394.18 cm**-1
45: 394.19 cm**-1
46: 398.57 cm**-1
47: 445.63 cm**-1
48: 445.64 cm**-1
49: 458.03 cm**-1
50: 459.39 cm**-1
51: 492.70 cm**-1
52: 494.00 cm**-1
53: 494.01 cm**-1

54: 499.35 cm**-1
55: 528.76 cm**-1
56: 528.77 cm**-1
57: 531.45 cm**-1
58: 532.08 cm**-1
59: 623.21 cm**-1
60: 623.47 cm**-1
61: 623.48 cm**-1
62: 624.58 cm**-1
63: 655.18 cm**-1
64: 655.18 cm**-1
65: 658.08 cm**-1
66: 658.52 cm**-1
67: 701.24 cm**-1
68: 701.28 cm**-1
69: 702.81 cm**-1
70: 702.96 cm**-1
71: 721.37 cm**-1
72: 721.78 cm**-1
73: 723.44 cm**-1
74: 723.46 cm**-1
75: 745.97 cm**-1
76: 745.98 cm**-1
77: 746.25 cm**-1
78: 746.39 cm**-1
79: 761.37 cm**-1
80: 761.38 cm**-1
81: 764.10 cm**-1
82: 764.31 cm**-1
83: 794.97 cm**-1
84: 795.24 cm**-1
85: 795.26 cm**-1
86: 795.37 cm**-1
87: 828.07 cm**-1
88: 828.18 cm**-1
89: 828.90 cm**-1
90: 828.95 cm**-1
91: 889.10 cm**-1
92: 889.11 cm**-1
93: 889.22 cm**-1
94: 889.36 cm**-1
95: 894.16 cm**-1
96: 894.18 cm**-1
97: 895.63 cm**-1
98: 895.69 cm**-1
99: 910.52 cm**-1
100: 910.96 cm**-1
101: 910.99 cm**-1
102: 910.99 cm**-1
103: 964.17 cm**-1
104: 964.78 cm**-1
105: 964.82 cm**-1
106: 967.60 cm**-1
107: 1001.34 cm**-1
108: 1001.35 cm**-1
109: 1001.39 cm**-1
110: 1001.51 cm**-1
111: 1018.07 cm**-1
112: 1018.08 cm**-1
113: 1019.07 cm**-1
114: 1019.13 cm**-1
115: 1019.96 cm**-1
116: 1020.46 cm**-1
117: 1020.49 cm**-1
118: 1021.06 cm**-1
119: 1053.34 cm**-1

120: 1053.37 cm**-1
121: 1053.63 cm**-1
122: 1053.93 cm**-1
123: 1070.60 cm**-1
124: 1070.61 cm**-1
125: 1072.34 cm**-1
126: 1072.47 cm**-1
127: 1081.79 cm**-1
128: 1084.07 cm**-1
129: 1085.06 cm**-1
130: 1085.07 cm**-1
131: 1123.03 cm**-1
132: 1124.60 cm**-1
133: 1124.76 cm**-1
134: 1124.86 cm**-1
135: 1160.27 cm**-1
136: 1160.41 cm**-1
137: 1160.43 cm**-1
138: 1164.41 cm**-1
139: 1165.76 cm**-1
140: 1166.58 cm**-1
141: 1166.60 cm**-1
142: 1166.94 cm**-1
143: 1195.28 cm**-1
144: 1195.29 cm**-1
145: 1198.74 cm**-1
146: 1203.85 cm**-1
147: 1290.35 cm**-1
148: 1290.83 cm**-1
149: 1292.47 cm**-1
150: 1292.50 cm**-1
151: 1306.72 cm**-1
152: 1306.74 cm**-1
153: 1309.27 cm**-1
154: 1309.60 cm**-1
155: 1311.65 cm**-1
156: 1311.71 cm**-1
157: 1315.86 cm**-1
158: 1318.59 cm**-1
159: 1363.11 cm**-1
160: 1363.12 cm**-1
161: 1363.40 cm**-1
162: 1367.36 cm**-1
163: 1438.25 cm**-1
164: 1438.27 cm**-1
165: 1438.40 cm**-1
166: 1438.48 cm**-1
167: 1457.29 cm**-1
168: 1459.75 cm**-1
169: 1461.74 cm**-1
170: 1461.75 cm**-1
171: 1475.79 cm**-1
172: 1476.90 cm**-1
173: 1476.98 cm**-1
174: 1477.02 cm**-1
175: 1498.58 cm**-1
176: 1498.59 cm**-1
177: 1502.20 cm**-1
178: 1502.99 cm**-1
179: 1584.78 cm**-1
180: 1585.86 cm**-1
181: 1586.34 cm**-1
182: 1586.36 cm**-1
183: 1605.22 cm**-1
184: 1605.43 cm**-1
185: 1606.31 cm**-1

186: 1606.31 cm**-1
187: 1657.98 cm**-1
188: 1658.00 cm**-1
189: 1658.42 cm**-1
190: 1658.57 cm**-1
191: 3200.91 cm**-1
192: 3200.94 cm**-1
193: 3200.95 cm**-1
194: 3200.98 cm**-1
195: 3216.44 cm**-1
196: 3216.46 cm**-1
197: 3216.49 cm**-1
198: 3216.60 cm**-1
199: 3222.12 cm**-1
200: 3222.18 cm**-1
201: 3222.20 cm**-1
202: 3222.22 cm**-1
203: 3228.93 cm**-1
204: 3228.97 cm**-1
205: 3229.09 cm**-1
206: 3229.12 cm**-1
207: 3229.46 cm**-1
208: 3229.49 cm**-1
209: 3229.57 cm**-1
210: 3229.60 cm**-1
211: 3243.06 cm**-1
212: 3243.16 cm**-1
213: 3243.18 cm**-1
214: 3243.19 cm**-1
215: 3263.31 cm**-1
216: 3263.32 cm**-1
217: 3263.44 cm**-1
218: 3263.54 cm**-1

S_4-symmetrized Coordinates from Chemcraft

Zr	0.000000000	0.000000000	0.000000000
N	-1.687635073	-1.262631826	-0.720776483
N	-1.215853466	-0.647409884	1.964050284
N	-1.262631826	1.687635073	0.720776483
N	0.647409884	-1.215853466	-1.964050284
N	1.687635073	1.262631826	-0.720776483
N	1.215853466	0.647409884	1.964050284
N	1.262631826	-1.687635073	0.720776483
N	-0.647409884	1.215853466	-1.964050284
C	-1.959009715	0.306980818	2.556919785
C	-1.393660798	2.990571131	0.323822546
H	-1.046216545	3.343703701	-0.479697552
C	-2.431961432	2.834822444	2.283273142
H	-2.914911540	3.039641877	3.068430728
C	-2.990571131	-1.393660798	-0.323822546
H	-3.343703701	-1.046216545	0.479697552
C	-1.912871319	1.599635193	1.925030612
C	-1.599635193	-1.912871319	-1.925030612
C	-0.306980818	-1.959009715	-2.556919785
C	-2.101379736	3.722278720	1.253557068
H	-2.321009460	4.644542862	1.205379965
C	-1.233341163	-1.892657563	2.476835368
H	-0.718363897	-2.564958405	2.059426826
C	-1.969350298	-2.232190646	3.583723407
H	-1.957783351	-3.119579010	3.921964864
C	1.892657563	-1.233341163	-2.476835368
H	2.564958405	-0.718363897	-2.059426826
C	-0.027683522	-2.730281308	-3.678946703
H	-0.709562638	-3.248952782	-4.080500328
C	-3.722278720	-2.101379736	-1.253557068

H	-4.644542862	-2.321009460	-1.205379965
C	-2.834822444	-2.431961432	-2.283273142
H	-3.039641877	-2.914911540	-3.068430728
C	-2.730281308	0.027683522	3.678946703
H	-3.248952782	0.709562638	4.080500328
C	-2.728630508	-1.250869753	4.195156959
H	-3.239372903	-1.458342087	4.958582750
C	2.232190646	-1.969350298	-3.583723407
H	3.119579010	-1.957783351	-3.921964864
C	1.250869753	-2.728630508	-4.195156959
H	1.458342087	-3.239372903	-4.958582750
C	1.959009715	-0.306980818	2.556919785
C	1.393660798	-2.990571131	0.323822546
H	1.046216545	-3.343703701	-0.479697552
C	2.431961432	-2.834822444	2.283273142
H	2.914911540	-3.039641877	3.068430728
C	2.990571131	1.393660798	-0.323822546
H	3.343703701	1.046216545	0.479697552
C	1.912871319	-1.599635193	1.925030612
C	1.599635193	1.912871319	-1.925030612
C	0.306980818	1.959009715	-2.556919785
C	2.101379736	-3.722278720	1.253557068
H	2.321009460	-4.644542862	1.205379965
C	1.233341163	1.892657563	2.476835368
H	0.718363897	2.564958405	2.059426826
C	1.969350298	2.232190646	3.583723407
H	1.957783351	3.119579010	3.921964864
C	-1.892657563	1.233341163	-2.476835368
H	-2.564958405	0.718363897	-2.059426826
C	0.027683522	2.730281308	-3.678946703
H	0.709562638	3.248952782	-4.080500328
C	3.722278720	2.101379736	-1.253557068
H	4.644542862	2.321009460	-1.205379965
C	2.834822444	2.431961432	-2.283273142
H	3.039641877	2.914911540	-3.068430728
C	2.730281308	-0.027683522	3.678946703
H	3.248952782	-0.709562638	4.080500328
C	2.728630508	1.250869753	4.195156959
H	3.239372903	1.458342087	4.958582750
C	-2.232190646	1.969350298	-3.583723407
H	-3.119579010	1.957783351	-3.921964864
C	-1.250869753	2.728630508	-4.195156959
H	-1.458342087	3.239372903	-4.958582750

8. References

(1) Rong, Y.; Al-Harbi, A.; Parkin, G. “Highly Variable Zr-CH2-Ph Bond Angles in Tetrabenzylzirconium: Analysis of Benzyl Ligand Coordination Modes.” *Organometallics* **2012**, *31*, 8208–8217.

(2) Ducloiset, C.; Jouin, P.; Paredes, E.; Guillot, R.; Sircoglou, M.; Orio, M.; Leibl, W.; Aukauloo, A. “Monoanionic Dipyrrin-Pyridine Ligands: Synthesis, Structure and Photophysical Properties.” *European Journal of Inorganic Chemistry* **2015**, *2015*, 5405–5410.

(3) Würth, C.; Grabolle, M.; Pauli, J.; Spieles, M.; Resch-Genger, U. “Relative and Absolute Determination of Fluorescence Quantum Yields of Transparent Samples.” *Nature Protocols* **2013**, *8*, 1535–1550.

(4) Neese, F.; Wennmohs, F.; Becker, U.; Riplinger, C. “The ORCA Quantum Chemistry Program Package.” *Journal of Chemical Physics* **2020**, *152*, 224108.

(5) Neese, F. “Software Update: The ORCA Program System—Version 5.0.” *WIREs Computational Molecular Science* **2022**.

(6) Lee, C.; Yang, W.; Parr, R. G. “Development of the Colle-Salvetti Correlation-Energy Formula into a Functional of the Electron Density.” *Physical Review B* **1988**, *37*, 785–789.

(7) Van Wüllen, C. “Molecular Density Functional Calculations in the Regular Relativistic Approximation:

Method, Application to Coinage Metal Diatomics, Hydrides, Fluorides and Chlorides, and Comparison with First-Order Relativistic Calculations." *Journal of Chemical Physics* **1998**, *109*, 392–399.
(8) Weigend, F.; Ahlrichs, R. "Balanced Basis Sets of Split Valence, Triple Zeta Valence and Quadruple Zeta Valence Quality for H to Rn: Design and Assessment of Accuracy." *Physical Chemistry Chemical Physics* **2005**, *7*, 3297–3305.
(9) Rolfes, J. D.; Neese, F.; Pantazis, D. A. "All-Electron Scalar Relativistic Basis Sets for the Elements Rb–Xe." *Journal of Computational Chemistry* **2020**, *41*, 1842–1849.
(10) Neese, F.; Wennmohs, F.; Hansen, A.; Becker, U. "Efficient, Approximate and Parallel Hartree-Fock and Hybrid DFT Calculations. A 'chain-of-Spheres' Algorithm for the Hartree-Fock Exchange." *Chemical Physics* **2009**, *356*, 98–109.
(11) Helmich-Paris, B.; de Souza, B.; Neese, F.; Izsák, R. "An Improved Chain of Spheres for Exchange Algorithm." *Journal of Chemical Physics* **2021**, *155*, 104109.
(12) Grimme, S.; Antony, J.; Ehrlich, S.; Krieg, H. "A Consistent and Accurate Ab Initio Parametrization of Density Functional Dispersion Correction (DFT-D) for the 94 Elements H-Pu." *Journal of Chemical Physics* **2010**, *132*, 180901.
(13) Grimme, S.; Ehrlich, S.; Goerigk, L. "Effect of the Damping Function in Dispersion Corrected Density Functional Theory." *Journal of Computational Chemistry* **2011**, *32*, 1456–1465.
(14) Garcia-Ratés, M.; Neese, F. "Effect of the Solute Cavity on the Solvation Energy and Its Derivatives within the Framework of the Gaussian Charge Scheme." *Journal of Computational Chemistry* **2020**, *41*, 922–939.
(15) Chemcraft https://www.chemcraftprog.com.